Valentina De Romeri
(CNRS - Laboratoire de Physique Corpusculaire Clermont-Ferrand)

Searches for new physics: lepton flavour phenomenology and indirect dark matter signatures

27th February 2015, LPC - Clermont

Based on works done in collaboration with
A. Abada, A. Teixeira, S.Monteil, J.Orloff, F. Calore, F. Donato,
M. Di Mauro, J. Herpich, A. Macció, L. Maccione, ...

Outline

1) New Physics Searches in Lepton Flavour

- Neutrino Masses and Mixings
- Inverse Seesaw (ISS)
- Sterile neutrinos
- Unitarity deviation
- Experimental constraints
- Numerical analysis
    - Inverse Seesaw (ISS)
    - "3+1" Effective model
- Lepton flavor conserving observables:
    - Lepton magnetic moments
    - Neutrinoless double beta decay
- Lepton flavor violating observables:
    - LFV Z decays at a high luminosity Z factory

2) Indirect searches for Dark Matter with gamma-rays
- Searches for WIMP dark matter
- Gamma-ray anisotropies from dark matter in the Milky Way: the role of the radial distribution

New physics beyond the SM?

The Higgs boson has been found, but no new particles have been found yet...

The Standard Model can explain most of the experimental results. However, there are some theoretical and observational issues to address.

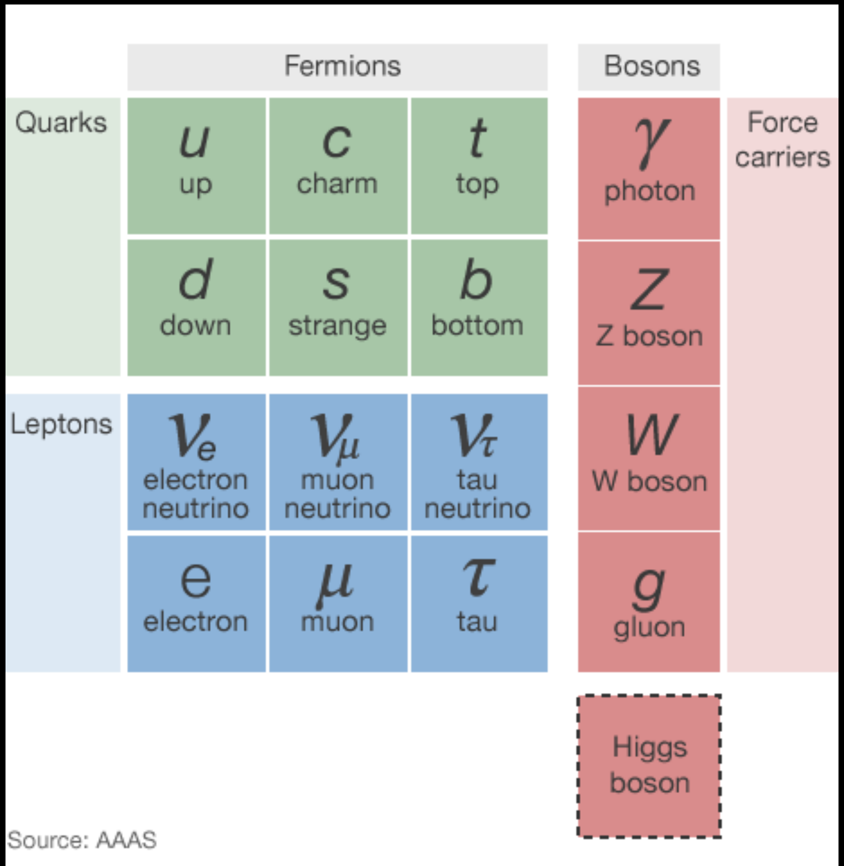

Unanswered questions: neutrino oscillations and DM (+ baryon asymmetry)

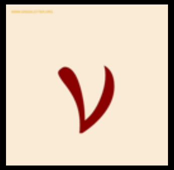

The Standard Model is considered to be incomplete: New Physics is needed.

1) New Physics Searches in Lepton Flavour

Neutrino physics

Although in the last years many pieces of the puzzle have been found, the neutrino physics picture is far from being complete.

As of today, data favour a three-active neutrinos oscillation framework, with very accurate measurements of the solar and atmospheric parameters.

Neutrino oscillation parameters have been inferred by detecting neutrinos coming from the Sun, the Earth's atmosphere, nuclear reactors and accelerator beams.

parameter	best fit ± 1σ	2σ range	3σ range
Δm^2_{21} $[10^{-5}\mathrm{eV}^2]$	$7.60^{+0.19}_{-0.18}$	7.26–7.99	7.11–8.18
$\lvert\Delta m^2_{31}\rvert$ $[10^{-3}\mathrm{eV}^2]$ (NH)	$2.48^{+0.05}_{-0.07}$	2.35–2.59	2.30–2.65
$\lvert\Delta m^2_{31}\rvert$ $[10^{-3}\mathrm{eV}^2]$ (IH)	$2.38^{+0.05}_{-0.06}$	2.26–2.48	2.20–2.54
$\sin^2\theta_{12}/10^{-1}$	3.23±0.16	2.92–3.57	2.78–3.75
$\theta_{12}/°$	34.6±1.0	32.7–36.7	31.8–37.8
$\sin^2\theta_{23}/10^{-1}$ (NH)	$5.67^{+0.32}_{-1.28}$ [a]	4.13–6.23	3.92 – 6.43
$\theta_{23}/°$	$48.9^{+1.9}_{-7.4}$	40.0–52.1	38.8–53.3
$\sin^2\theta_{23}/10^{-1}$ (IH)	$5.73^{+0.25}_{-0.43}$	4.32–6.21	4.03–6.40
$\theta_{23}/°$	$49.2^{+1.5}_{-2.5}$	41.1–52.0	39.4–53.1
$\sin^2\theta_{13}/10^{-2}$ (NH)	2.34±0.20	1.95–2.74	1.77–2.94
$\theta_{13}/°$	8.8±0.4	8.0–9.5	7.7–9.9
$\sin^2\theta_{13}/10^{-2}$ (IH)	2.40±0.19	2.02–2.78	1.83–2.97
$\theta_{13}/°$	8.9±0.4	8.2–9.6	7.8–9.9
δ/π (NH)	$1.34^{+0.64}_{-0.38}$	0.0–2.0	0.0–2.0
$\delta/°$	241^{+115}_{-68}	0–360	0–360
δ/π (IH)	$1.48^{+0.34}_{-0.32}$	0.0–0.14 & 0.81-2.0	0.0–2.0
$\delta/°$	266^{+61}_{-58}	0–25 & 146–360	0–360

[a] There is a local minimum in the first octant, $\sin^2\theta_{23} = 0.467$ with $\Delta\chi^2 = 0.28$ with respect to the global minimum

(Forero et al., arXiv:1405.7540)

Solar $\nu_e \rightarrow \nu_{\mu,\tau}$ SNO, BOREXino, Super-Kamiokande, GALLEX/GNO, SAGE, Homestake, Kamiokande

Atmospheric $\nu_\mu \rightarrow \nu_\tau$, LBL Accelerator ν_μ disappearance, LBL Accelerator
IMB, MAcro, Soudan-2, Kamiokande, Super-Kamiokande

LBL Accelerator ($\nu_\mu \rightarrow \nu_e$), LBL Reactor ($\overline{\nu}$ disappearance)
T2K, MINOS Daya Bay, RENO, Double Chooz

SBL Accelerator (ν_μ ($\overline{\nu}_\mu$) $\rightarrow$ ν_e ($\overline{\nu}_e$)), SBL Reactor ($\overline{\nu}$ disappearance)
LSND, MiniBooNE, ++ Solar: GALLEX, SAGE++Bugey, ILL, Rovno..

Neutrino physics open questions

Among the missing ingredients there are:

- Absolute mass scale (Tritium β decays: $m_{\nu e}$<2.05eV, Cosmology: $\sum m_{\nu i}$<0.66 eV (CMB), $\sum m_{\nu i}$<0.23 eV (CMB+BAO+WMAP polarization data+high-resolution CMB experiments and flat Universe)) (Troitsk and Mainz, Planck 2013)
- Majorana versus Dirac nature (0νββ decay) (KamLAND-Zen,EXO-200,Gerda)
- The mass ordering (normal or inverted "hierarchy") (matter effects in sun and long baseline oscillations, T2K,NOvA...)
- Is there CP violation in the lepton sector?
- Are there extra sterile states?
- What is the underlying mechanism responsible for the generation of their masses?

In the SM, neutrinos are strictly massless:

- absence of RH neutrino fields ➟ no Dirac mass term (no renormalizable mass term)
- no Higgs triplet ➟ no Majorana mass term (would break the electroweak gauge symmetry, because it is not invariant under the weak isospin symmetry; does not conserve the lepton number L)

Massive neutrinos require BSM physics

Several models of neutrino mass generation:

- Seesaw mechanism: Type-I, Type-II,Type-III, low-scale seesaws (Inverse seesaw, Linear seesaw, νMSM) etc ...
- Radiative models

...

(Minkowski 77, Gell-Mann Ramond Slansky 80, Glashow, Yanagida 79,Mohapatra Senjanovic 80,Lazarides Shafi Wetterich 81, Schechter-Valle, 80 & 82, Mohapatra Senjanovic 80,Lazarides 80,Foot 88, Ma, Hambye et al., Bajc, Senjanovic, Lin, Abada et al., Notari et al…)

Inverse seesaw (Mohapatra & Valle, 1986)

Add three generations of SM singlet pairs, ν_R and X (with L=+1)

Inverse seesaw basis (ν_L,ν_R,X)

$$M^\nu = \begin{pmatrix} 0 & m_D & 0 \\ m_D^T & 0 & M_R \\ 0 & M_R^T & \mu_X \end{pmatrix}$$

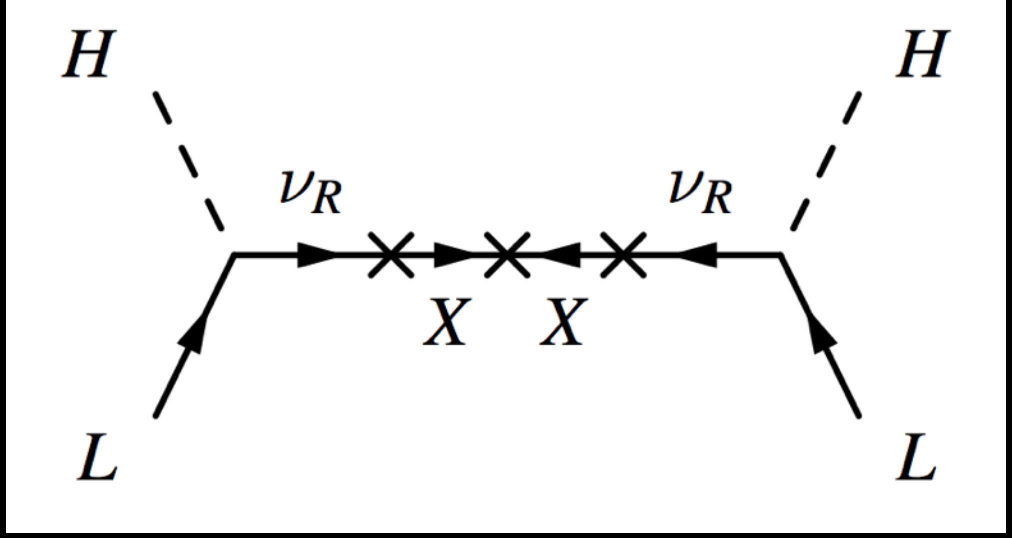

After EWSB the effective light neutrino masses are given by

$$m_\nu = m_D (M_R^T)^{-1} \mu_X (M_R)^{-1} m_D^T$$

$Y_\nu \sim O(1)$ and $M_R \sim$ 1TeV testable at the colliders and low energy experiments.

Large mixings (active-sterile) and light sterile neutrinos are possible

Sterile neutrinos

From the invisible decay width of the Z boson [LEP]:
⇒ extra neutrinos must be sterile (=EW singlets) or cannot be a Z decay product

Any singlet fermion that mixes with the SM neutrinos
• Right-handed neutrinos • Other singlet fermions

Sterile neutrinos are SM gauge singlets - only interact via their mixing with the active ones

Several oscillation results or anomalies (reactor antineutrino anomaly, LSND, MiniBooNe...) cannot be explained within 3-flavor oscillations
⇒ need at least an extra neutrino

Other motivations for sterile neutrinos from cosmology, e.g. keV sterile neutrino as warm dark matter or to explain pulsar velocities

Active-sterile mixing

Leptonic charged currents can be modified due to the mixing with the steriles.

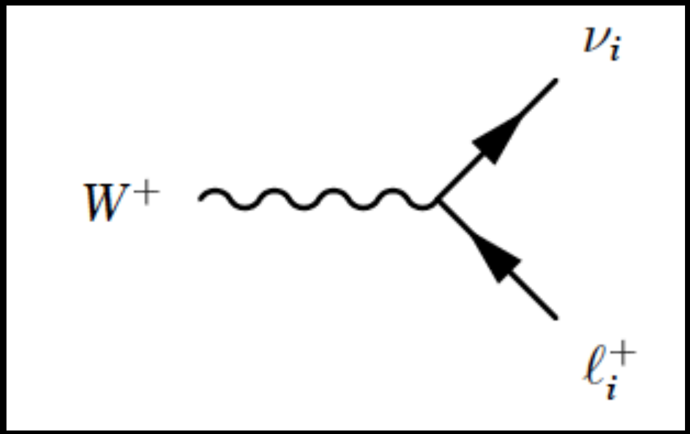

Active-sterile mixing

Leptonic charged currents can be modified due to the mixing with the steriles.

Standard case (3 flavors):

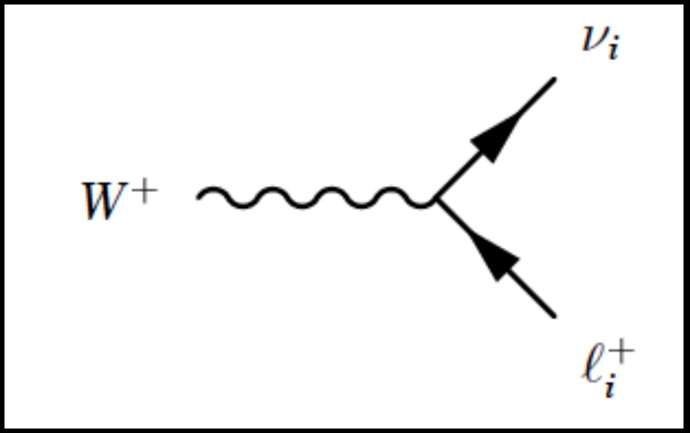

ν_i = e,μ,τ

ν_i = flavor eigenstate = $\sum_{ai} U_{ai}^{PMNS}\, \nu_a$

ν_a = mass eigenstates, a = 1,2,3

Add sterile neutrinos:

$$-\mathcal{L}_{cc} = \frac{g}{\sqrt{2}} U^{ji} \bar{l}_j \gamma^\mu P_L \nu_i W^-_\mu + \text{c.c.}$$

$\nu_i = \sum_{ai} U_{ai}\, \nu_a$, a = 1,2,3,4 ..9..$n_\nu$ U = extended matrix, j=1…3, i=1…n_ν

If $n_\nu > 3$, $U \neq U_{PMNS}$ → the 3x3 sub matrix is not unitary

$$U_{\rm PMNS} \;\rightarrow\; \tilde{U}_{\rm PMNS} \;=\; (\mathbb{1} - \eta)\, U_{\rm PMNS}$$

(see also: Fernandez-Martinez et al. 2007, Gavela et al. 2009, Abada et al. 2014, Arganda et al. 2014)

Experimental constraints

The deviations from unitarity and the possibility of having steriles as final decay products, might induce departures from the SM expectations.

1. Neutrino oscillation parameters (seesaw approximation and PMNS)
2. Unitarity constraints
3. Electroweak precision data
4. LHC data (invisible decays)
5. Leptonic and semileptonic meson decays (B and D)
6. Laboratory bounds: direct searches for sterile neutrinos
7. Lepton flavor violation ($\mu \to e \gamma$)
8. Neutrinoless double beta decay
9. Cosmological bounds on sterile neutrinos

Experimental constraints

1. Neutrino oscillation parameters (seesaw approximation and PMNS)
2. Unitarity constraints

Non-standard neutrino interactions with matter can be generated by NP.

$$U_{3\times 3} = (1-\eta)U_{PMNS}$$

effective theory approach

(Antusch et al., 2009)

3. Electroweak precision data
4. LHC data (invisible decays)
5. Leptonic and semileptonic meson decays (B and D)
6. Laboratory bounds: direct searches for sterile neutrinos
7. Lepton flavor violation ($\mu \to e\,\gamma$)
8. Neutrinoless double beta decay
9. Cosmological bounds on sterile neutrinos

Experimental constraints

1. Neutrino oscillation parameters (seesaw approximation and PMNS)
2. Unitarity constraints

   Non-standard neutrino interactions with matter can be generated by NP.

   $$U_{3\times3} = (1-\eta)U_{PMNS}$$

   effective theory approach
3. Electroweak precision data

   invisible and leptonic Z-decay widths, the Weinberg angle and the values of g_L and g_R

(Del Aguila et al., 2008, Atre et al., 2009)

4. LHC data (invisible decays)
5. Leptonic and semileptonic meson decays (B and D)
6. Laboratory bounds: direct searches for sterile neutrinos
7. Lepton flavor violation ($\mu \to e\,\gamma$)
8. Neutrinoless double beta decay
9. Cosmological bounds on sterile neutrinos

Experimental constraints

1. Neutrino oscillation parameters (seesaw approximation and PMNS)
2. Unitarity constraints

   Non-standard neutrino interactions with matter can be generated by NP.

   $U_{3\times 3} = (1-\eta)U_{PMNS}$

   effective theory approach
3. Electroweak precision data

   invisible and leptonic Z-decay widths, the Weinberg angle and the values of g_L and g_R
4. LHC data (invisible decays)

   decay modes of the Higgs boson

   $h \to \nu_R\, \nu_L$ relevant for sterile neutrino masses ~100 GeV

   (Bhupal Dev et al., 2012, P. Bandyopadhyay et al,2012, Cely et al., 2013,Arganda et al. 2014)
5. Leptonic and semileptonic meson decays (B and D)
6. Laboratory bounds: direct searches for sterile neutrinos
7. Lepton flavor violation ($\mu \to e\, \gamma$)
8. Neutrinoless double beta decay
9. Cosmological bounds on sterile neutrinos

Experimental constraints

1. Neutrino oscillation parameters (seesaw approximation and PMNS)
2. Unitarity constraints

   Non-standard neutrino interactions with matter can be generated by NP.

   $U_{3\times 3} = (1-\eta)U_{PMNS}$

   effective theory approach
3. Electroweak precision data

   invisible and leptonic Z-decay widths, the Weinberg angle and the values of g_L and g_R
4. LHC data (invisible decays)

   decay modes of the Higgs boson $h \to \nu_R\, \nu_L$ relevant for sterile neutrino masses ~100 GeV
5. Leptonic and semileptonic meson decays (K,B and D)

   $\Gamma(P \to l\nu)$ with P = K,D,B with one or two neutrinos in the final state

   (J. Beringer et al. ,PDG, 2013)

6. Laboratory bounds: direct searches for sterile neutrinos
7. Lepton flavor violation ($\mu \to e\,\gamma$)
8. Neutrinoless double beta decay
9. Cosmological bounds on sterile neutrinos

Experimental constraints

1. Neutrino oscillation parameters (seesaw approximation and PMNS)
2. Unitarity constraints

   Non-standard neutrino interactions with matter can be generated by NP.

   $U_{3\times3} = (1-\eta)U_{PMNS}$

   effective theory approach
3. Electroweak precision data

   invisible and leptonic Z-decay widths, the Weinberg angle and the values of g_L and g_R
4. LHC data (invisible decays)

   decay modes of the Higgs boson

   $h \to \nu_R \nu_L$ relevant for sterile neutrino masses ~100 GeV
5. Leptonic and semileptonic meson decays (K,B and D)

   $\Gamma(P \to l\nu)$ with P = K,D,B with one or two neutrinos in the final state
6. Laboratory bounds: direct searches for sterile neutrinos

   e.g. $\pi^\pm \to \mu^\pm \nu_S$, the lepton spectrum would show a monochromatic line.

   (Atre et al. 2009, Kusenko et al. 2009)
7. Lepton flavor violation ($\mu \to e\,\gamma$)
8. Neutrinoless double beta decay
9. Cosmological bounds on sterile neutrinos

Experimental constraints

1. Neutrino oscillation parameters (seesaw approximation and PMNS)
2. Unitarity constraints

   Non-standard neutrino interactions with matter can be generated by NP.

   $U_{3\times3} = (1-\eta)U_{PMNS}$

   effective theory approach
3. Electroweak precision data

   invisible and leptonic Z-decay widths, the Weinberg angle and the values of g_L and g_R
4. LHC data (invisible decays)

   decay modes of the Higgs boson

   $h \to \nu_R\, \nu_L$ relevant for sterile neutrino masses ~100 GeV
5. Leptonic and semileptonic meson decays (K,B and D)

   $\Gamma(P \to l\nu)$ with P = K,D,B with one or two neutrinos in the final state
6. Laboratory bounds: direct searches for sterile neutrinos

   e.g. $\pi^\pm \to \mu^\pm \nu_S$, the lepton spectrum would show a monochromatic line.
7. Lepton flavor violation ($\mu \to e\, \gamma$)

   $Br(\mu \to e\gamma)_{MEG} = 0.57 \times 10^{-12}$

   (Ilakovac and Pilaftsis,1995, Deppisch and Valle, 2005)

8. Neutrinoless double beta decay
9. Cosmological bounds on sterile neutrinos

Experimental constraints

1. Neutrino oscillation parameters (seesaw approximation and PMNS)
2. Unitarity constraints — Non-standard neutrino interactions with matter can be generated by NP. $U_{3\times3} = (1-\eta)U_{PMNS}$ effective theory approach
3. Electroweak precision data — invisible and leptonic Z-decay widths, the Weinberg angle and the values of g_L and g_R
4. LHC data (invisible decays) — decay modes of the Higgs boson $h \to \nu_R\, \nu_L$ relevant for sterile neutrino masses ~100 GeV
5. Leptonic and semileptonic meson decays (K,B and D) — $\Gamma(P \to l\nu)$ with P = K,D,B with one or two neutrinos in the final state
6. Laboratory bounds: direct searches for sterile neutrinos — e.g. $\pi^\pm \to \mu^\pm \nu_S$, the lepton spectrum would show a monochromatic line.
7. Lepton flavor violation ($\mu \to e\, \gamma$) $Br(\mu \to e\gamma)_{MEG} = 0.57 \times 10^{-12}$

9. Neutrinoless double beta decay $m_\nu^{\beta\beta} = \sum_i U_{ei}^2 m_i \leq (140-700) meV$ (EXO-200,KamLAND-Zen,GERDA,CUORICINO)

(see also: Blennow et al. 2010, Lopez-Pavon et al. 2013, Abada et al. 2014)

10. Cosmological bounds on sterile neutrinos

Experimental constraints

1. Neutrino oscillation parameters (seesaw approximation and PMNS)
2. Unitarity constraints — Non-standard neutrino interactions with matter can be generated by NP. $U_{3\times3} = (1-\eta)U_{PMNS}$ effective theory approach
3. Electroweak precision data — invisible and leptonic Z-decay widths, the Weinberg angle and the values of g_L and g_R
4. LHC data (invisible decays) — decay modes of the Higgs boson $h \to \nu_R\, \nu_L$ relevant for sterile neutrino masses ~100 GeV
5. Leptonic and semileptonic meson decays (K,B and D) — $\Gamma(P \to l\nu)$ with P = K,D,B with one or two neutrinos in the final state
6. Laboratory bounds: direct searches for sterile neutrinos — e.g. $\pi^{\pm} \to \mu^{\pm}\nu_S$, the lepton spectrum would show a monochromatic line.
7. Lepton flavor violation ($\mu \to e\,\gamma$) $Br(\mu \to e\gamma)_{MEG} = 0.57 \times 10^{-12}$

9. Neutrinoless double beta decay $m_\nu^{\beta\beta} = \sum_i U_{ei}^2 m_i \leq (140-700)meV$

10. Cosmological bounds on sterile neutrinos — Large scale structure, Lyman-α, BBN, CMB, X-ray constraints (from $\nu_i \to \nu_j\gamma$),SN1987a

(Smirnov et al. 2006, Kusenko 2009, Gelmini 2010)

Numerical analysis:
Inverse Seesaw and Effective "3+1" model

Inverse Seesaw

couplings Yv can be written using a modified Casas-Ibarra parametrization

$$Y_\nu = \frac{\sqrt{2}}{v} D^\dagger \mathrm{diag}(\sqrt{\mathrm{M}}) \mathrm{R} \mathrm{diag}(\sqrt{\mathrm{m}_\nu}) \mathrm{U}^\dagger_{\mathrm{PMNS}} \qquad M = M_R \frac{1}{\mu_X} M_R^T$$

basis (ν_L,ν_R,X)

$$M^\nu = \begin{pmatrix} 0 & m_D & 0 \\ m_D^T & 0 & M_R \\ 0 & M_R^T & \mu_X \end{pmatrix}$$

diagonalised by 9x9 complex matrix U_ν

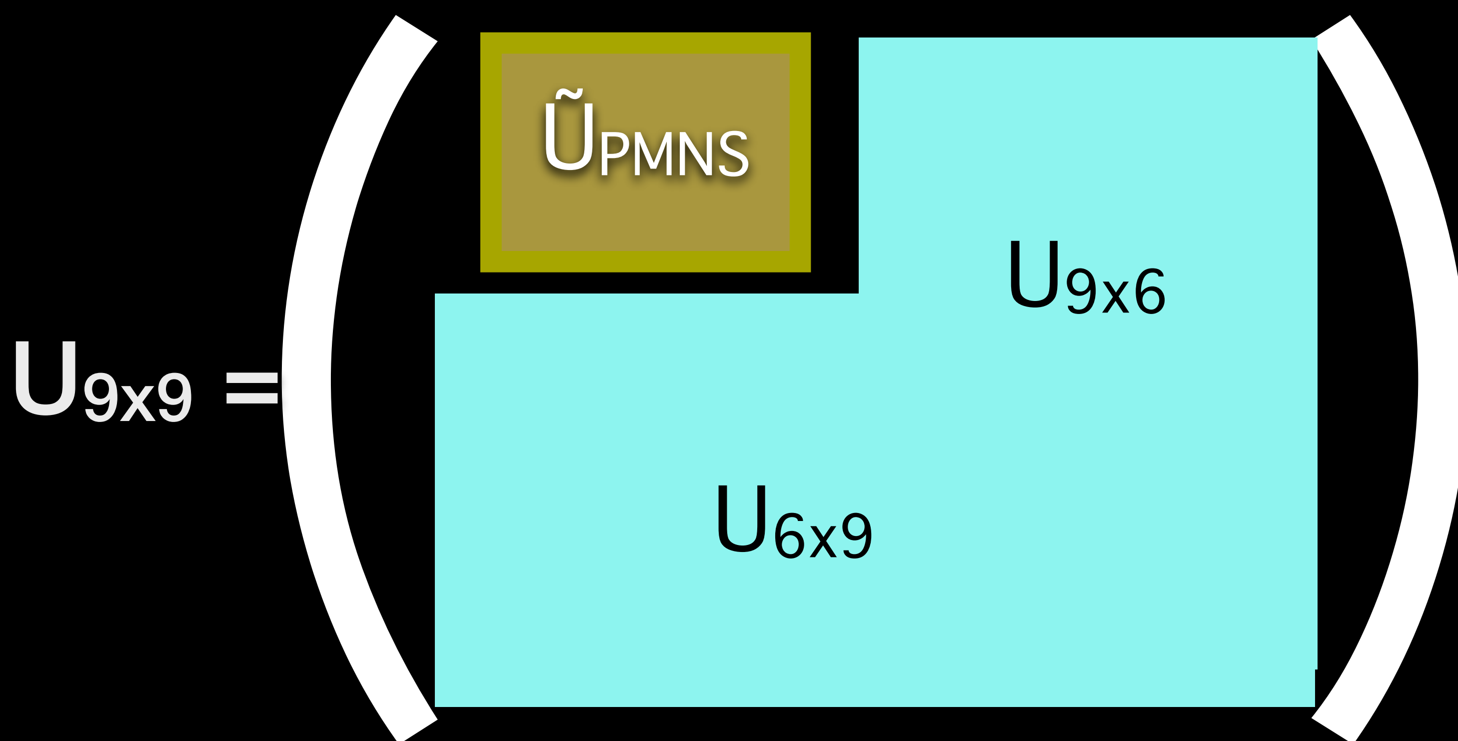

Parameters:

- M_R (real, diagonal) M_R = (0.1 MeV, 10^6 GeV)
- μ_X (complex,symmetric) μ_X = (0.01 eV, 1 MeV)
- R_{mat} (rotation,complex)
- 2 Majorana and 1 Dirac phases from U_{PMNS}
- Normal (NH) / Inverted (IH) hierarchy

Effective model: 3+1

Add a sterile state → 3 new mixing angles actives-sterile

$$U_{4\times 4} = R_{34}.R_{24}.R_{14}.\boxed{R_{23}.R_{13}.R_{12}}$$

U_{PMNS}

U_{4x4} =

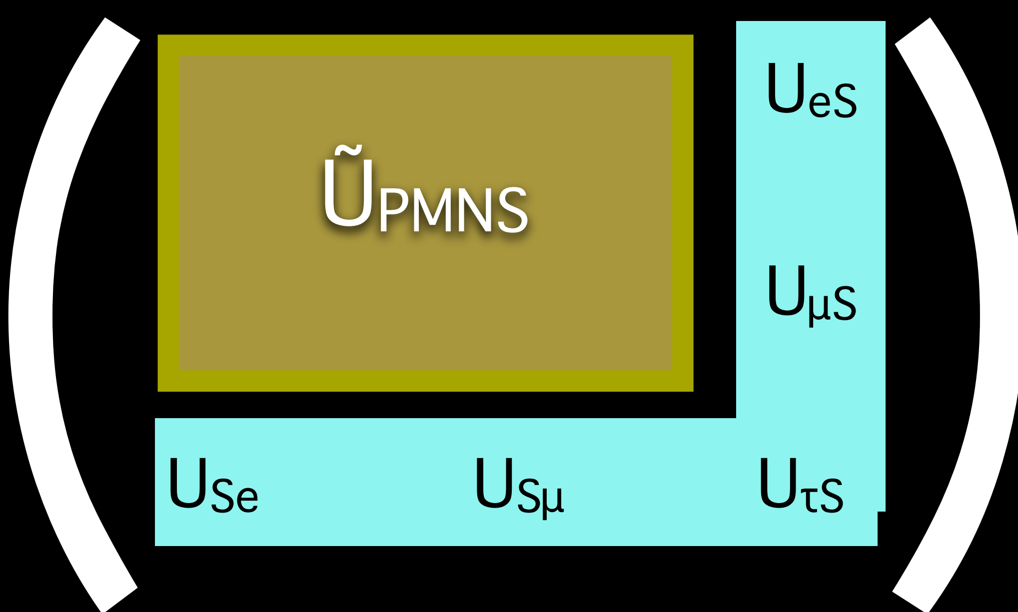

Parameters:

- $\theta_{14}, \theta_{24}, \theta_{34}$
- 3 Majorana and 3 Dirac phases
- Normal (NH) / Inverted (IH) hierarchy

Lepton flavor conserving observables: lepton magnetic moments and neutrinoless double beta decay

(Abada, VDR, Teixeira, JHEP 09 (2014) 074)

Lepton magnetic moments

The Dirac theory predicts a magnetic dipole moment in the presence of an external magnetic field, for any lepton (l=e,μ,τ)

$$\vec{M} = g_\ell \frac{q}{2m_\ell} \vec{S}$$

with gyromagnetic ratio $g_\ell = 2$

Quantum loop effects lead to a small calculable deviation, which is parametrized by the anomalous magnetic moment (g-2)

$$g_\ell = 2(1 + a_\ell)$$

$$a_l = a_l^{QED} + a_l^{EW} + a_l^{had} + a_l^{NP}$$

$$\Delta a_e = a_e^{exp} - a_e^{SM} = -10.5(8.1) \times 10^{-13}$$

$$\Delta a_\mu = a_\mu^{exp} - a_\mu^{SM} = 288(63)(49) \times 10^{-11}$$

(J. Beringer et al. PDG, 2013)

Effective "3+1": a_e

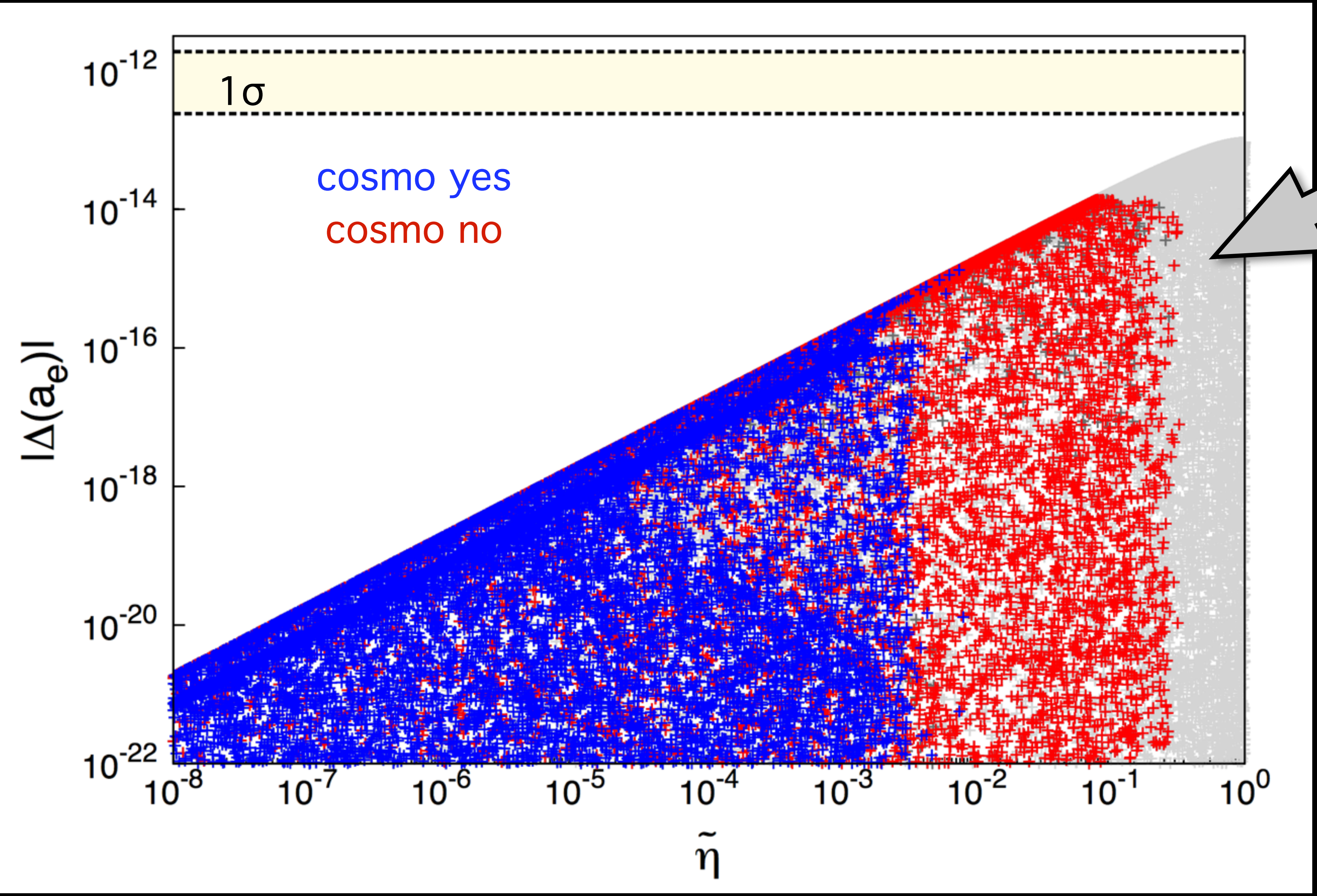

mainly excluded by ν oscillation data and lab bounds

$$\tilde{\eta} = 1 - \det(\tilde{U}_{PMNS})$$

measures the deviation from unitarity.

No relevant contribution $\Delta(a_e)$: no new constraint on the model

Effective "3+1": a_μ

$$\tilde{\eta} = 1 - \det(\tilde{U}_{PMNS})$$

measures the deviation from unitarity.

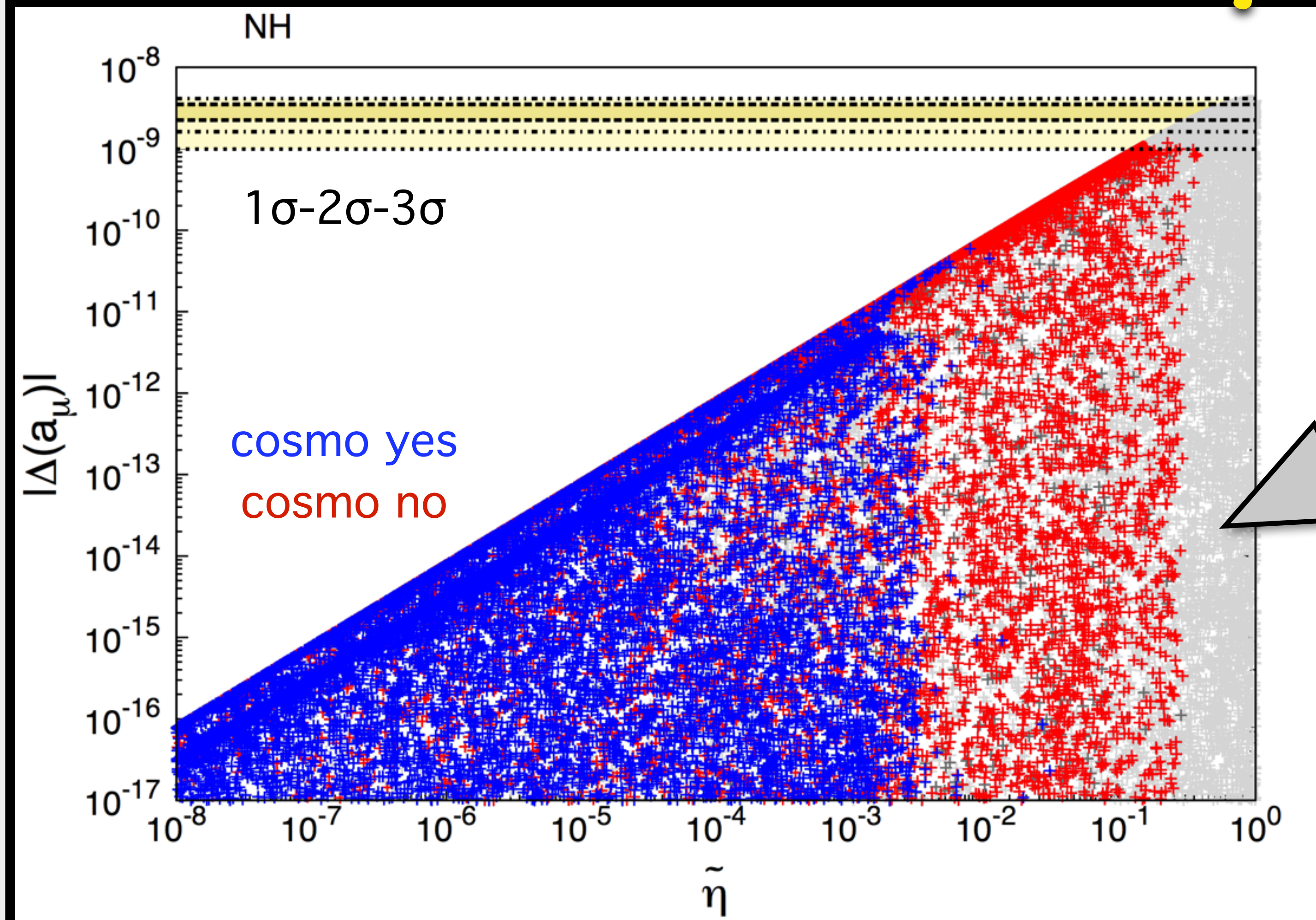

mainly excluded by
ν oscillation data
and lab bounds

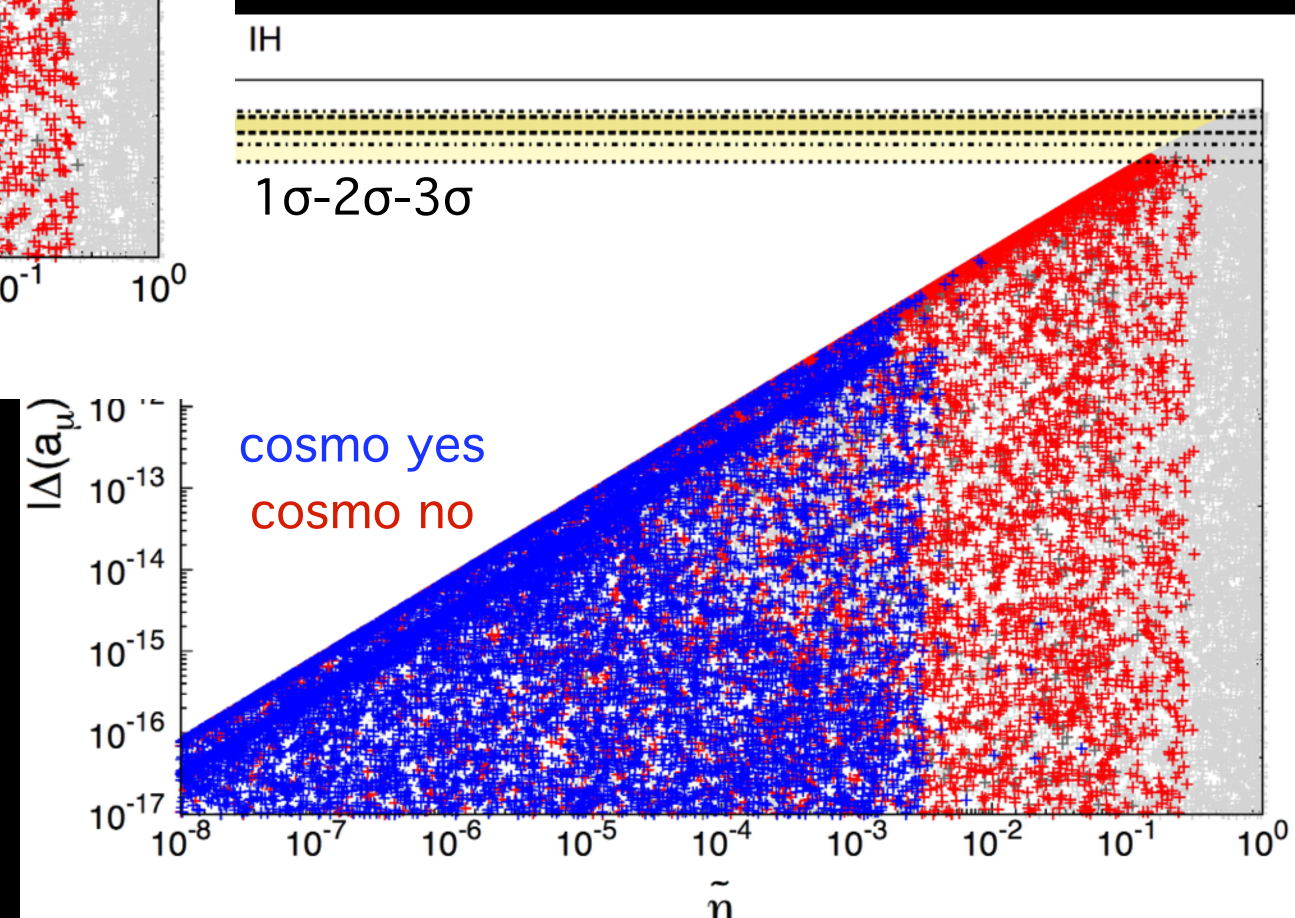

- Constraint from active neutrino oscillations (entries of U_{PMNS}) rules out most solutions with large $\hat{\eta}$

Effective "3+1": 0νββ decay

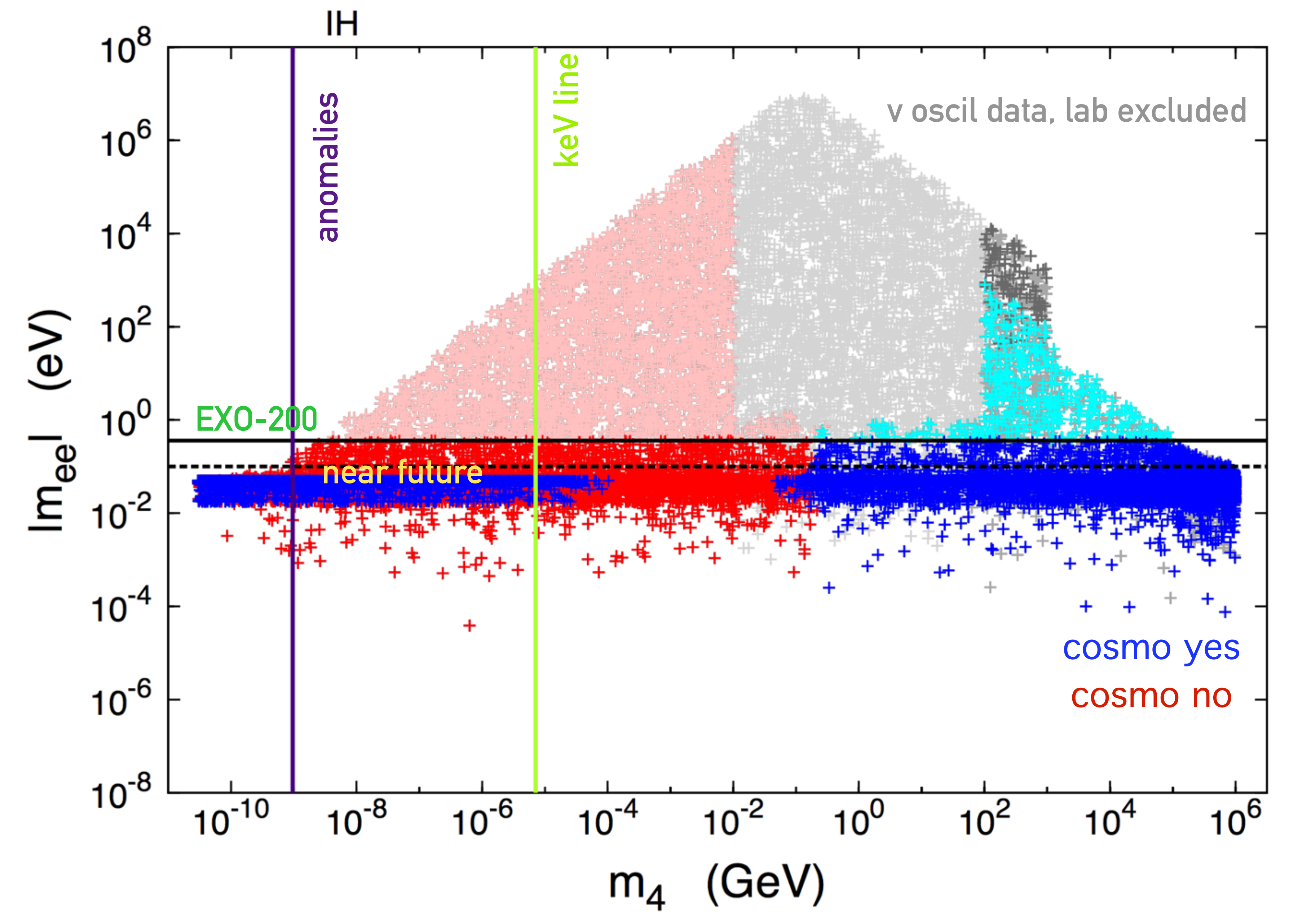

$$m_{ee} \simeq \sum_{i=1}^{4} U_{ei}^2 \, p^2 \frac{m_i}{p^2 - m_i^2}$$

p: momentum exchanged in the process ($p^2 \sim -(100\text{ MeV})^2$ virtual momentum of the neutrino)

We also studied effective masses $|m_{\mu\mu}|$ and $|m_{e\mu}|$, no significant contribution.

ISS: a_μ

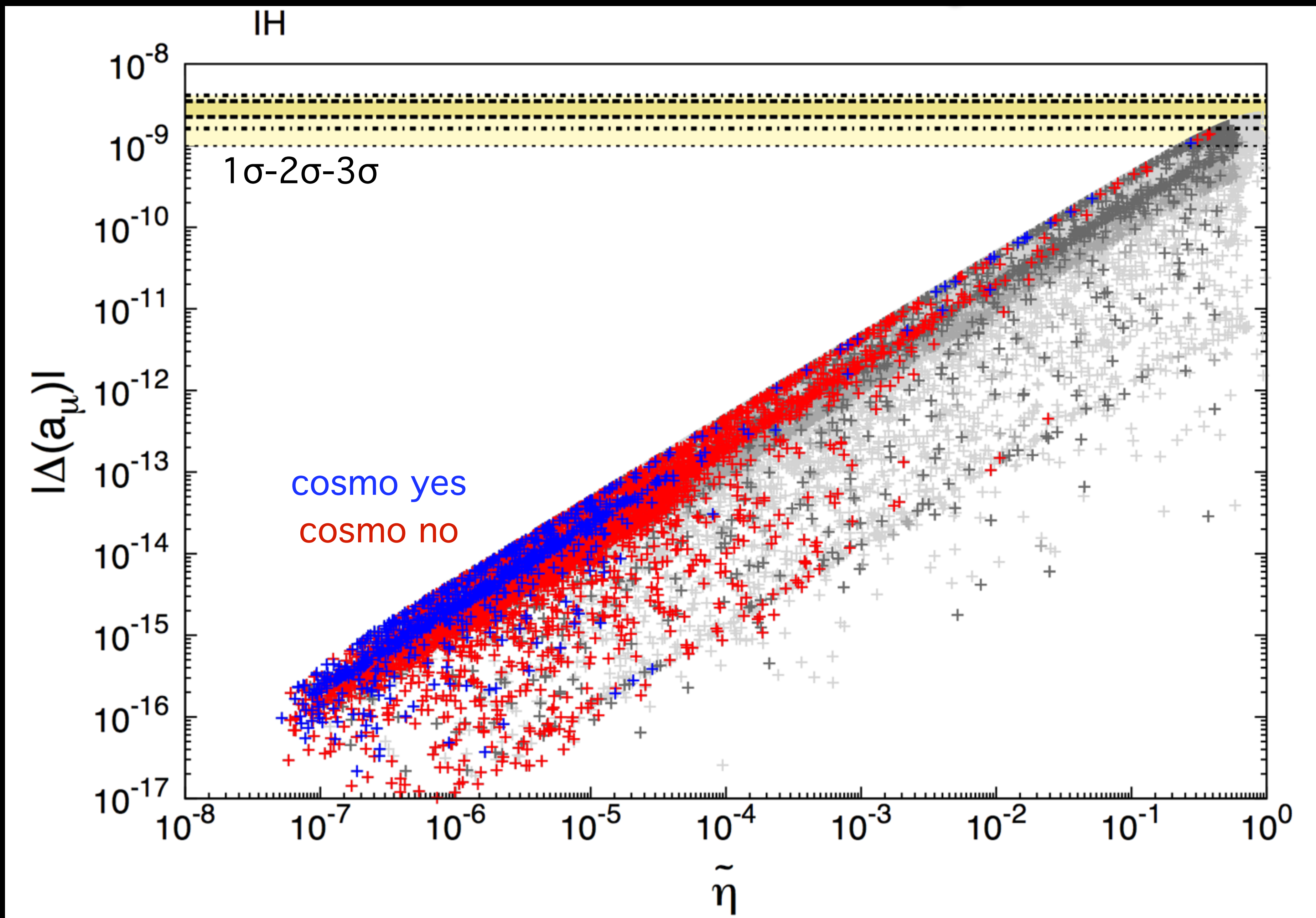

$$\tilde{\eta} = 1 - \det(\tilde{\mathrm{U}}_{\mathrm{PMNS}})$$

measures the deviation from unitarity.

For large $\hat{\eta}$ we can get points with a_μ within 3σ of the expected value

ISS: 0νββ decay

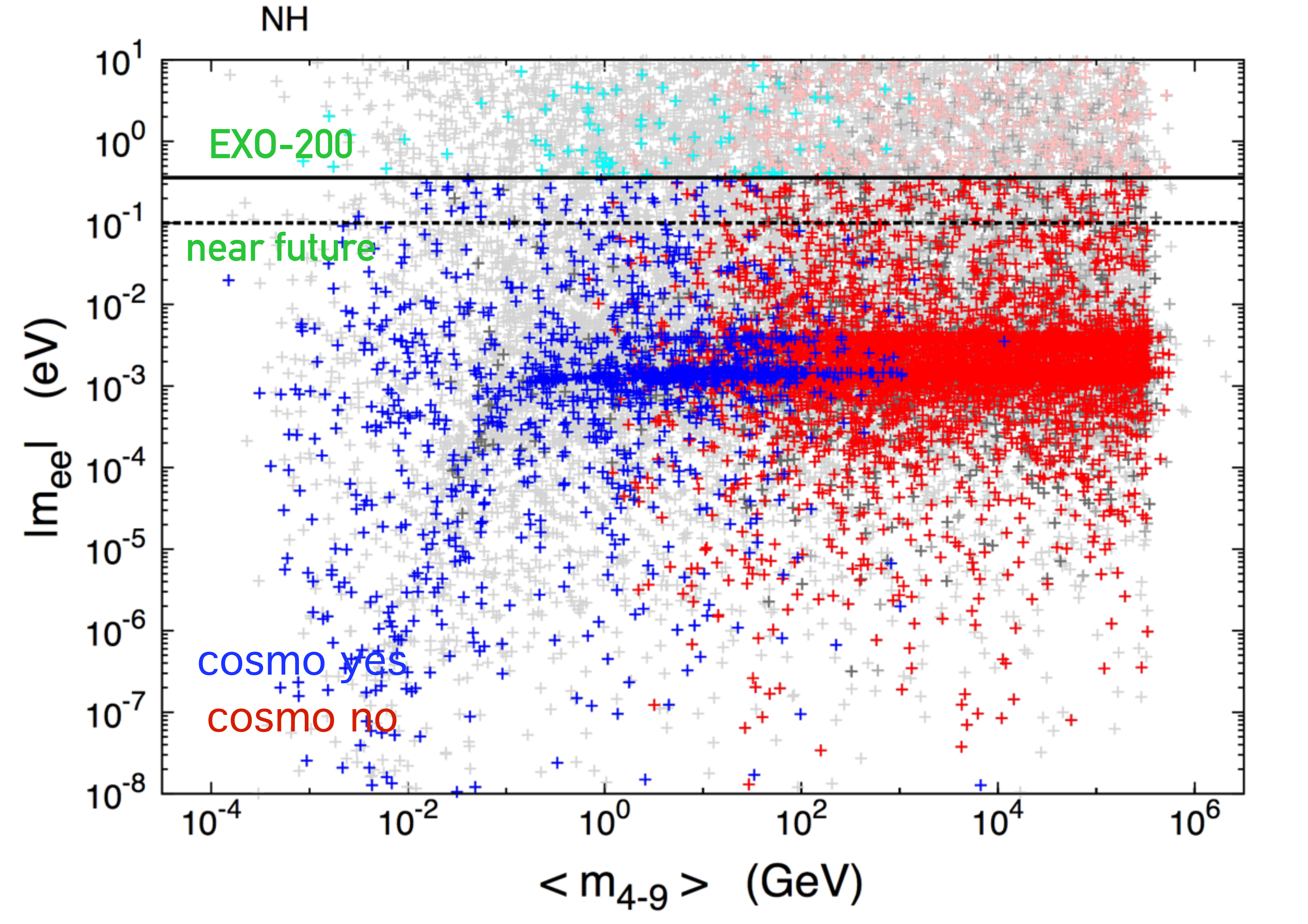

p: momentum exchanged in the process

$m_s \ll |p|$: in this regime the effective mass goes to zero

$$m^{\nu_e}_{\text{eff}} = p^2 \sum_{i=1}^{7} U^2_{e,i} \frac{m_i}{p^2 - m_i^2} \simeq \sum_{i=1}^{7} U^2_{e,i}\, m_i$$

$m_s \approx |p|$: the contribution of the pseudo-Dirac states becomes more important, and can induce sizeable effects to m_{ee}

$m_s \gg |p|$: in this regime the heavy states decouple, and the contributions to m_{ee} only arise from the 3 light neutrino states.

$$m_\nu^{\beta\beta} = \sum_i U_{ei}^2 p^2 \frac{m_i}{p^2 - m_i^2}$$

- 0νββ decay excludes some solutions
- points within the reach of actual and near-future experiments

Lepton flavor violating observables:
LFV Z decays
at a high luminosity Z-factory

(Abada, VDR, Monteil, Orloff, Teixeira, arXiv:1412.6322, accepted by JHEP)

Future circular (and linear) colliders

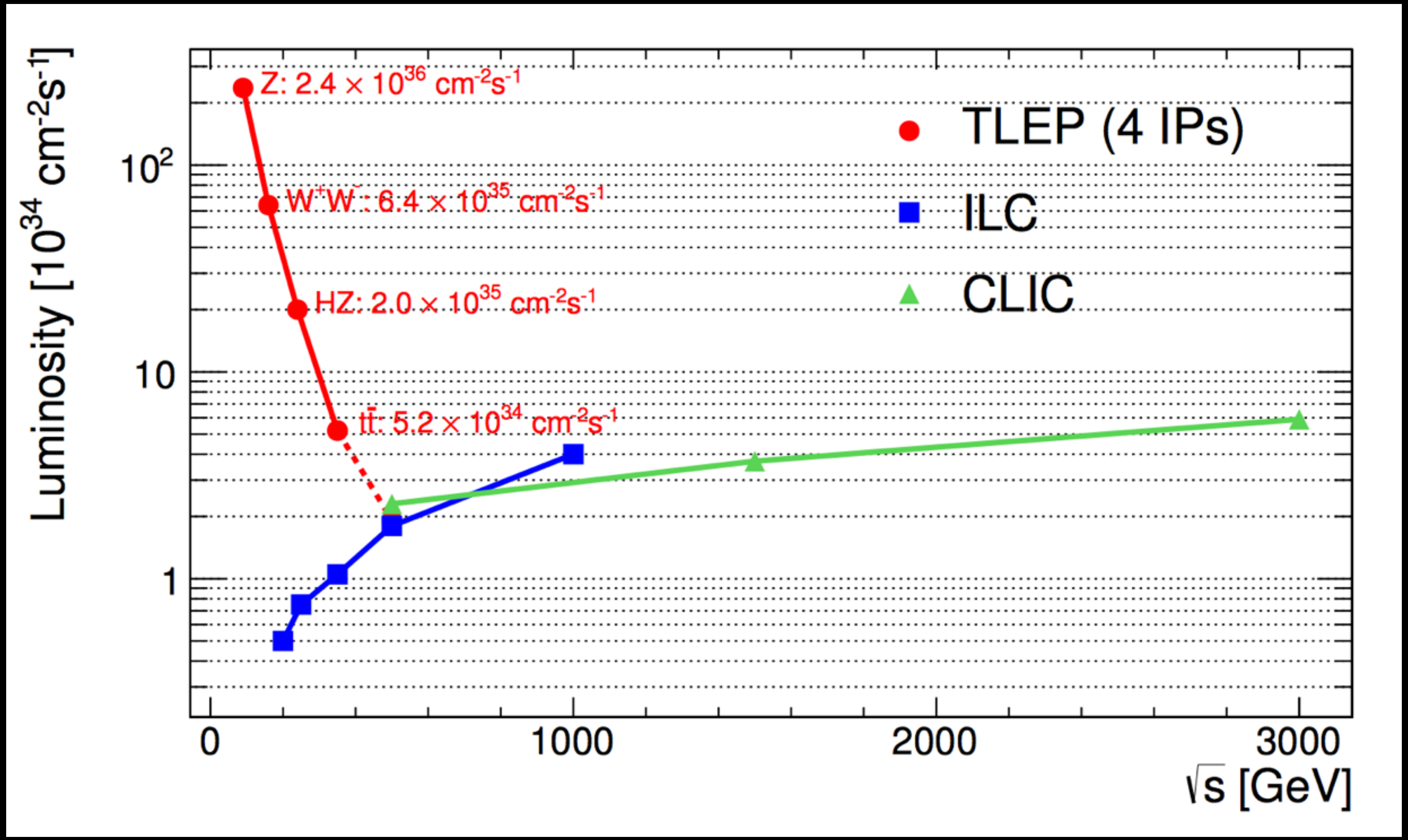

Instantaneous luminosity expected at FCC-ee, in a configuration with four interaction points operating simultaneously, as a function of the centre-of-mass energy.

FCC-ee is designed to provide e^+e^- collisions in the beam energy range of 40 to 175 GeV.

What would we like see with 10^{12} Z?

New physics effects in rare Z decays

In the SM with lepton mixing (U_{PMNS}) the theoretical predictions are:

$$BR(Z \to e^{\pm}\mu^{\mp}) \sim BR(Z \to e^{\pm}\tau^{\mp}) \sim 10^{-54}$$

$$BR(Z \to \mu^{\pm}\tau^{\mp}) \sim 4 \times 10^{-60}$$

The detection of a rare decay as $Z \to l_i^{\mp} l_j^{\pm}$ (i≠j) would serve as an indisputable evidence of new physics

Current limits:

$$\begin{array}{lcl} \mathrm{BR}(Z \to e^{\mp}\mu^{\pm}) & < & 1.7 \times 10^{-6} \\ \mathrm{BR}(Z \to e^{\mp}\tau^{\pm}) & < & 9.8 \times 10^{-6} \\ \mathrm{BR}(Z \to \mu^{\mp}\tau^{\pm}) & < & 1.2 \times 10^{-5} \end{array}$$

$$\mathrm{Br}\,(Z \to e\mu) < 7.5 \cdot 10^{-7}$$

OPAL Collaboration, R. Akers et al., Z. Phys. C67 (1995) 555–564.
L3 Collaboration, O. Adriani et al., Phys. Lett. B316 (1993) 427.
DELPHI Collaboration, P. Abreu et al., Z. Phys. C73 (1997) 243.
ATLAS, CERN-PH-EP-2014-195 (2014)

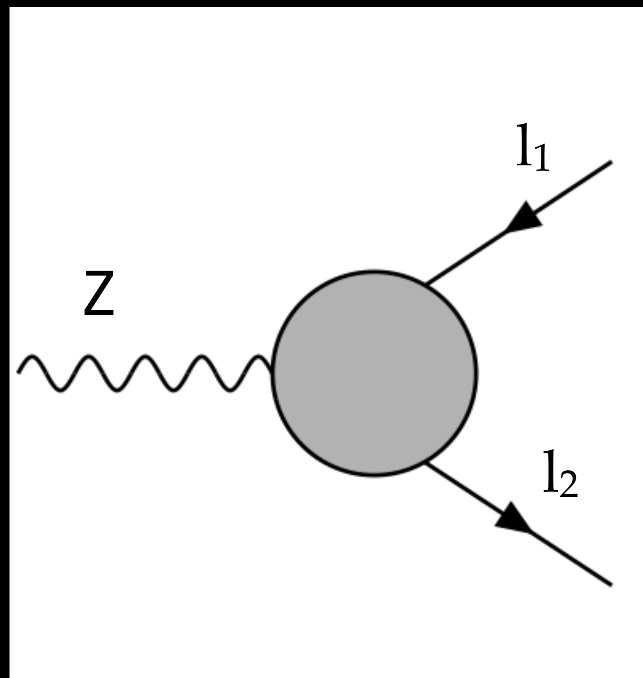

ν_i are physical states, $i = 3+N$

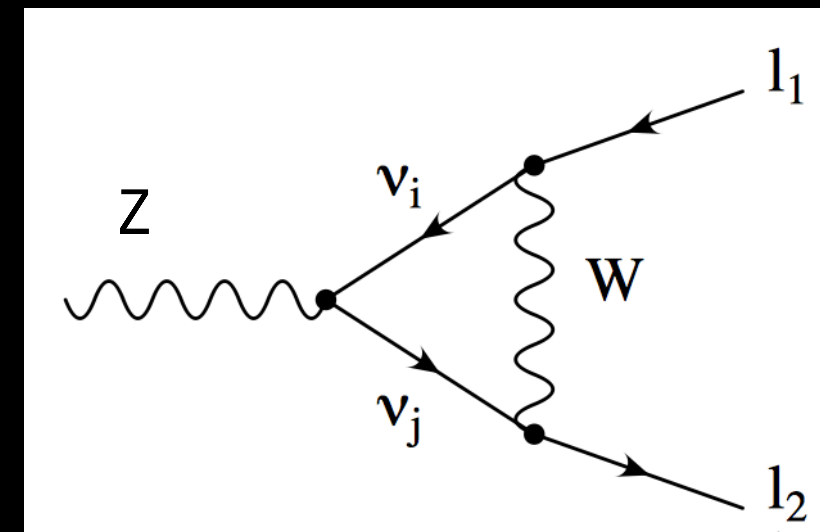

N = extra Majorana states
(m ~ 10^{-10} - 10^{3} GeV)

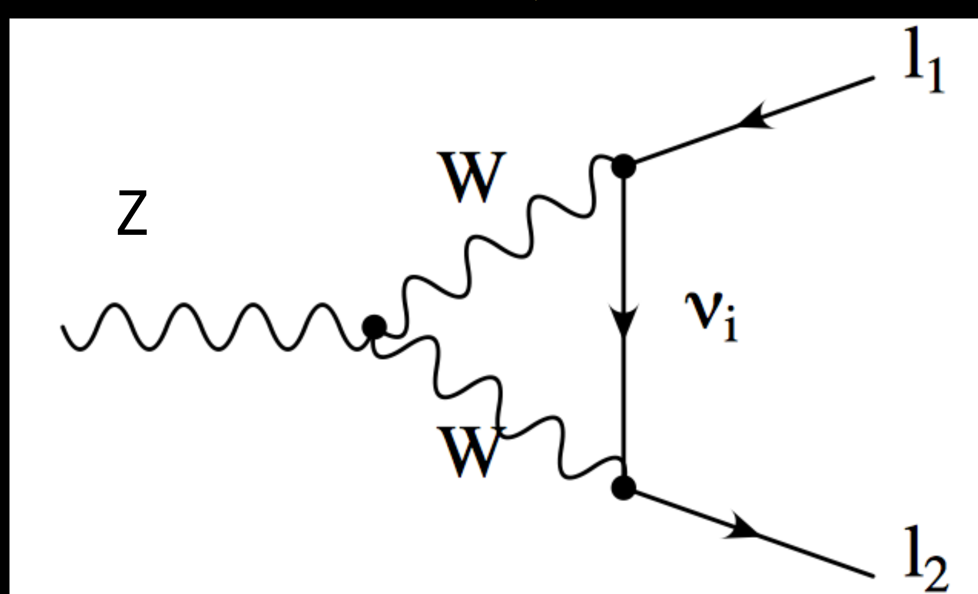

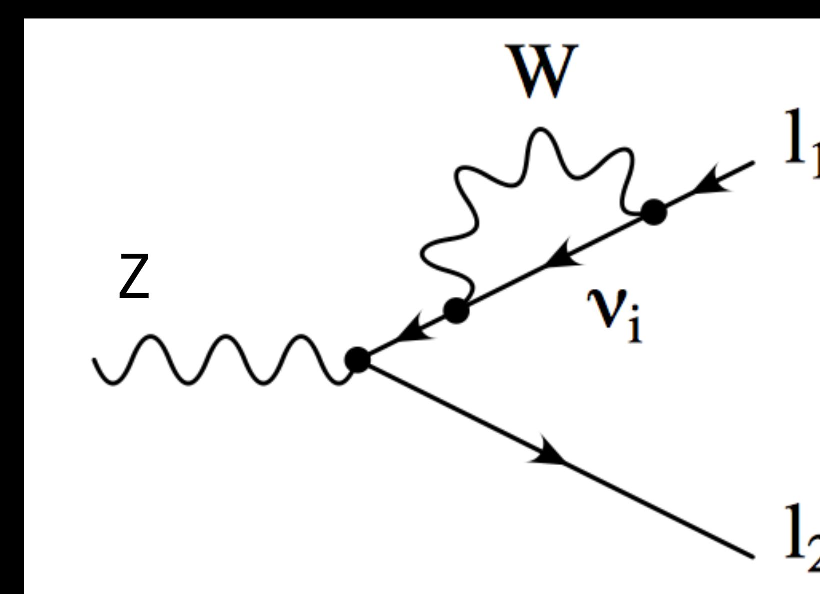

Effective "3+1": $Z \to e^{\pm}\mu^{\mp}$ vs $\mu \to e$ conversion in Al

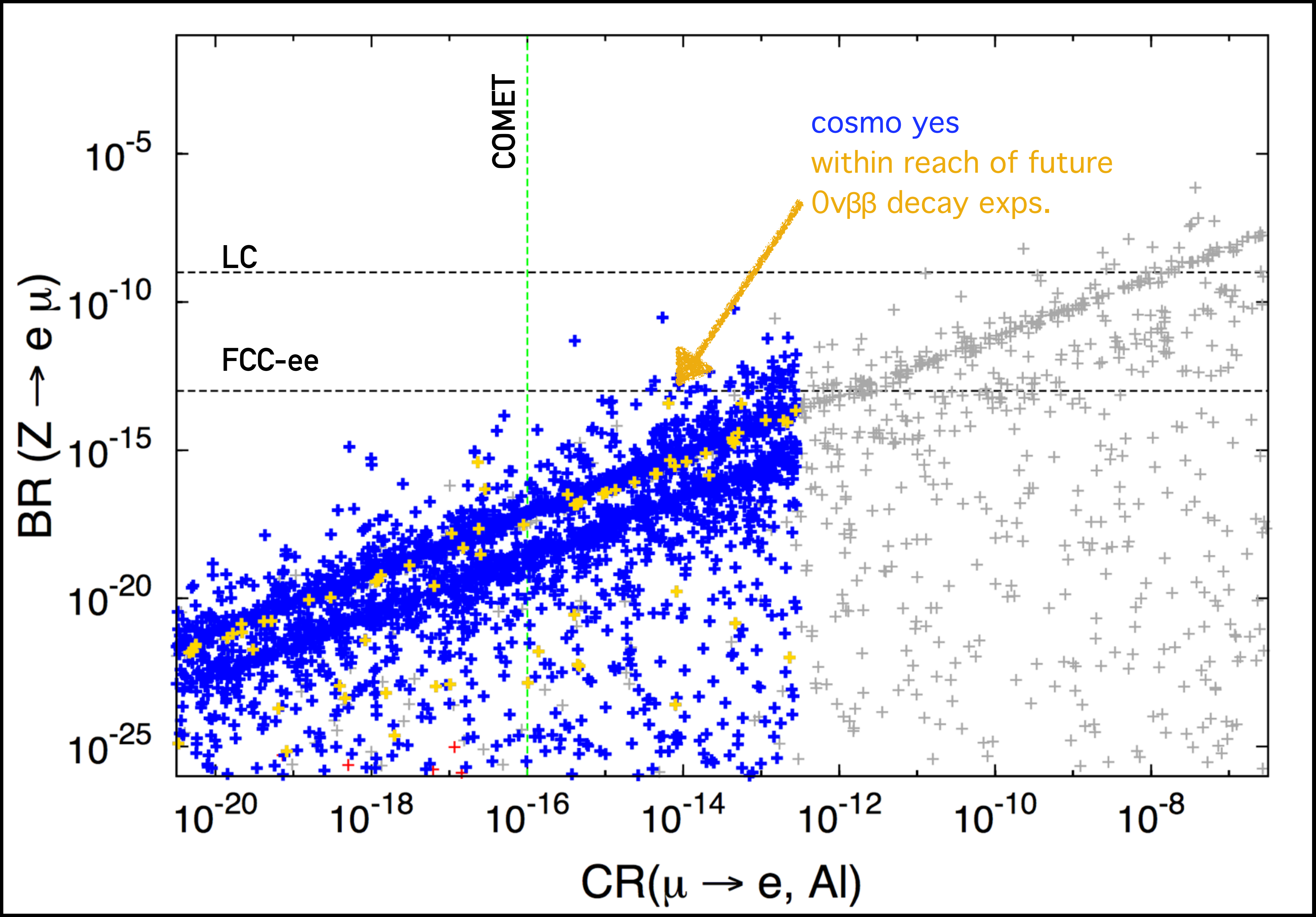

Effective "3+1": $Z \to \tau^{\pm}\mu^{\mp}$ vs $\tau \to \mu\mu\mu$

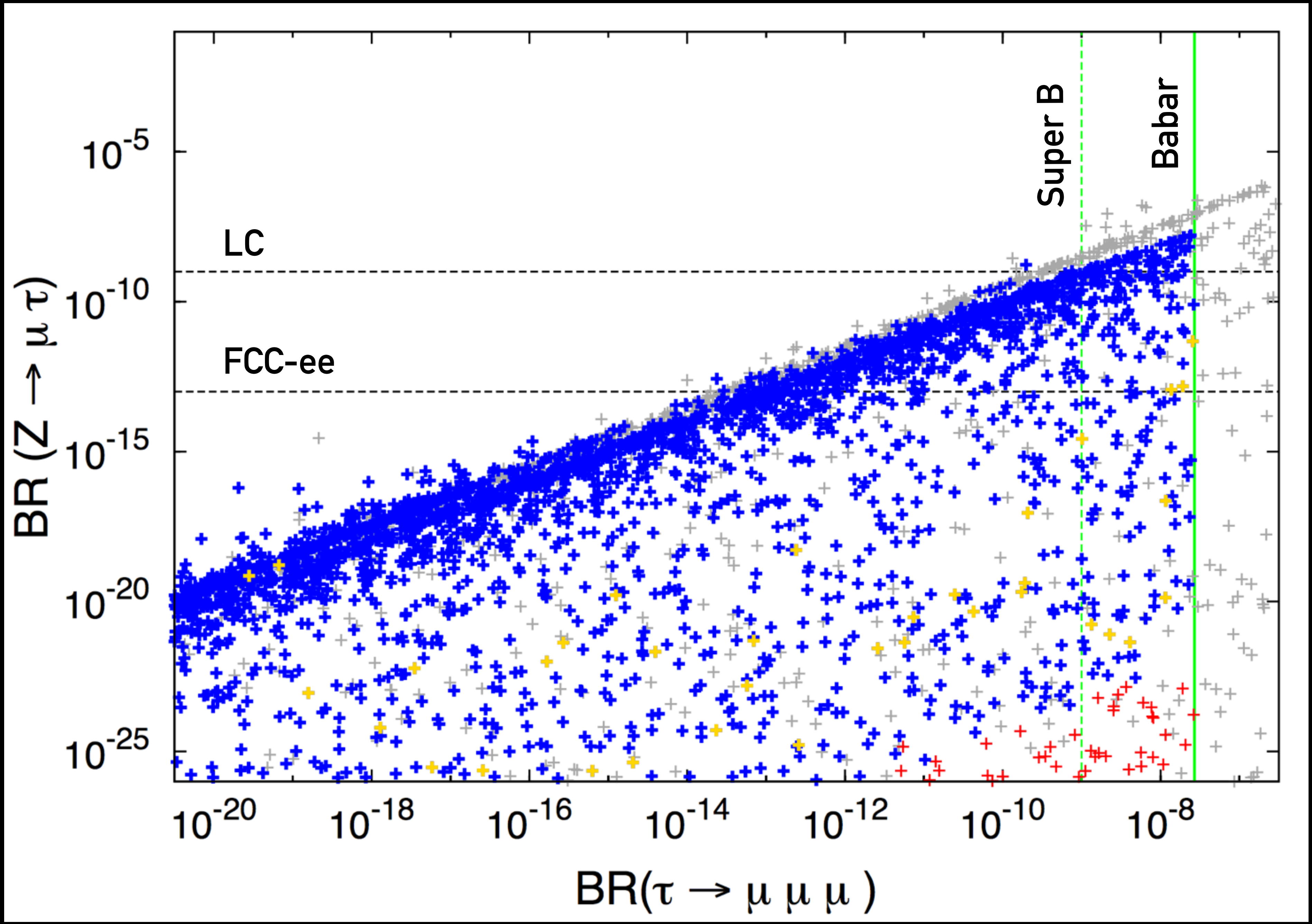

Effective "3+1": $Z \to \tau^{\pm}\mu^{\mp}$ vs $\tau \to \mu\gamma$

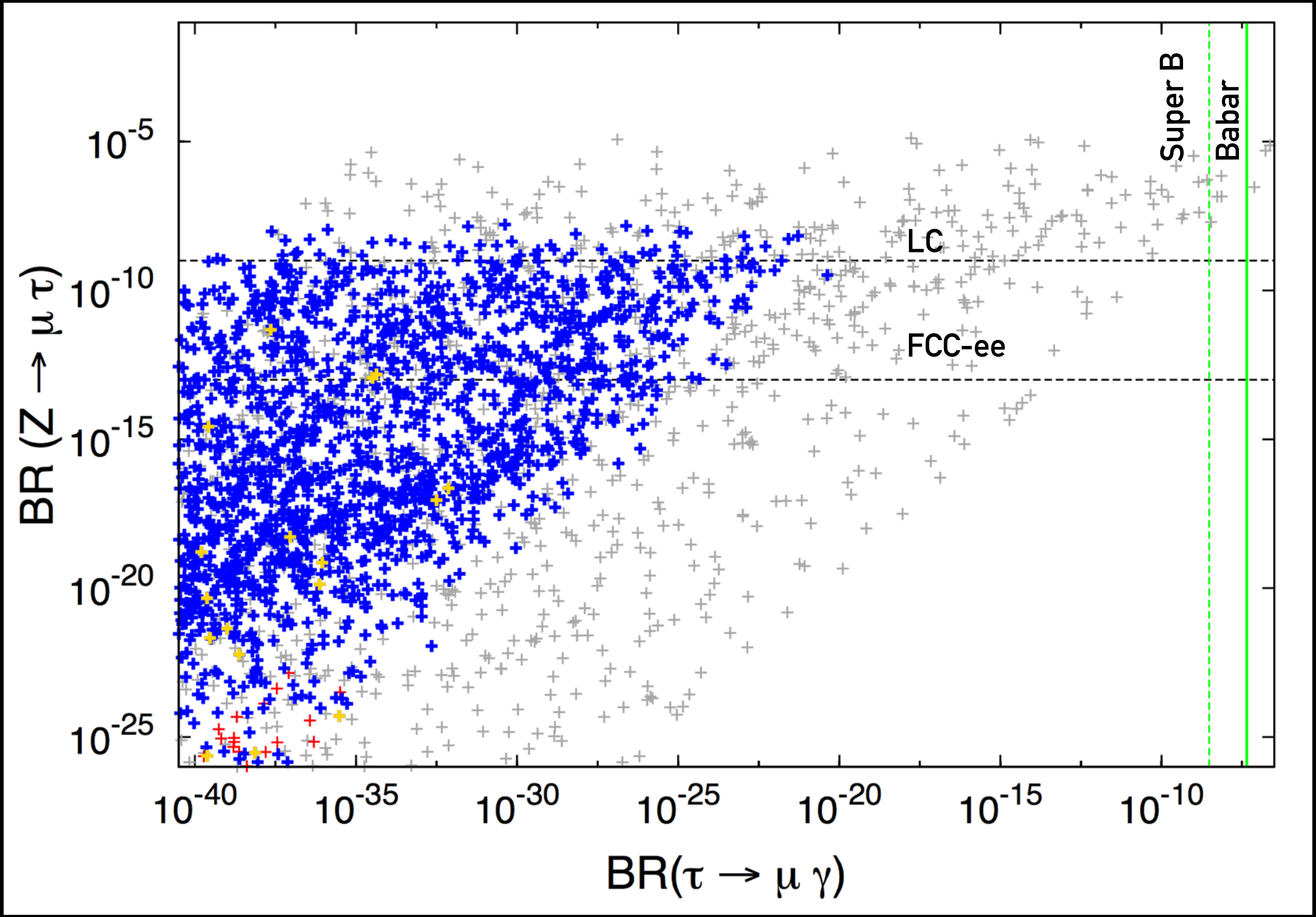

ISS: $Z \rightarrow \mu^{\pm}\tau^{\mp}$

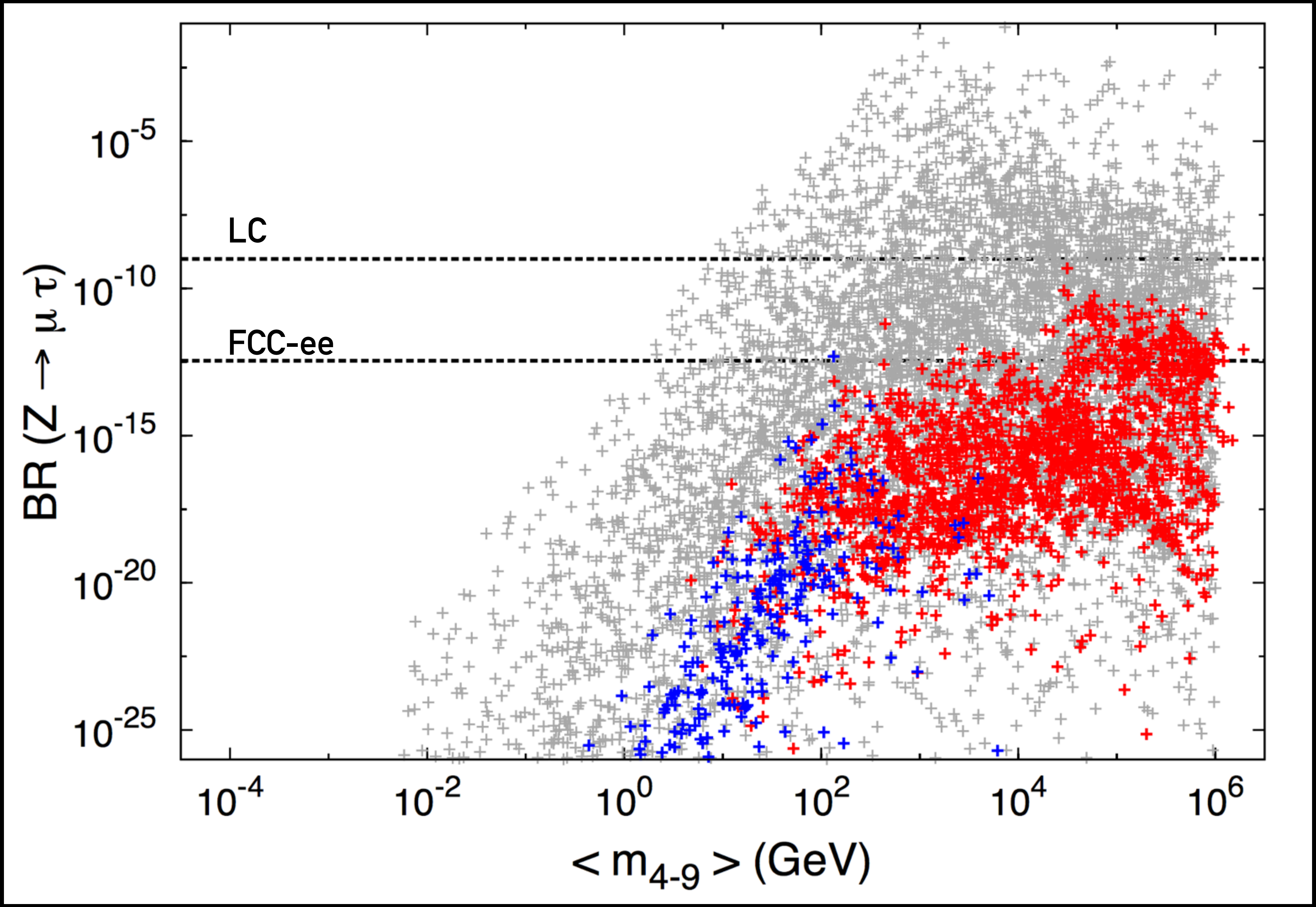

Conclusions - LFV

We have considered two extensions of the SM (ISS and 3+1) which add to the particle content of the SM one or more sterile neutrinos.

We have investigated the contribution of the sterile states to the anomalous magnetic moment of the leptons in these two classes of models and discussed them taking into account a number of experimental and theoretical constraints.

Even if the scale of such NP is low, its contribution to the anomalous magnetic moment of the leptons is generically smaller than the errors in theoretical calculation. However, for large η (deviation from unitarity) we can get solutions within 3σ of the expectation. The largest mixing angles (active-sterile) which would give a sizeable contribution to the muon g-2 are indeed strongly constrained by other EW observables, among which $0\nu\beta\beta$.

Concerning rare LFV Z decays, we have seen that a future high-luminosity Z factory has the power to probe LFV especially in the μ-τ sector, in complementarity to the reach of low energy exps.

A non negligible region of the parameter space of both models has also the potential to account for signals in three distinct facilities (low E facilities, LFV Z decays and $0\nu\beta\beta$).

2) Indirect searches for Dark Matter through gamma-rays

There is overwhelming evidence for the existence of dark matter:

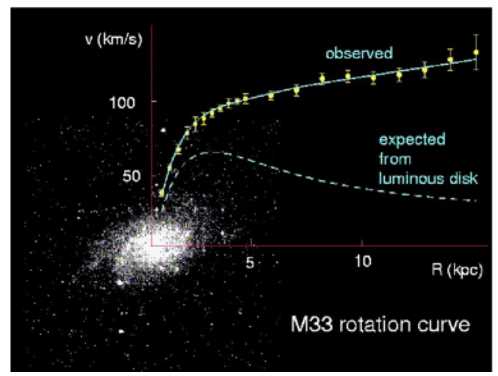

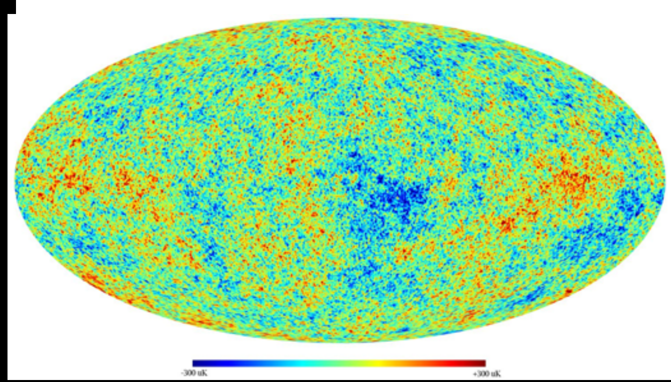

CMB anisotropies,
Clusters (X-rays, lensing),
Large Scale Structures,
Galaxies (rotation curves, fits...)

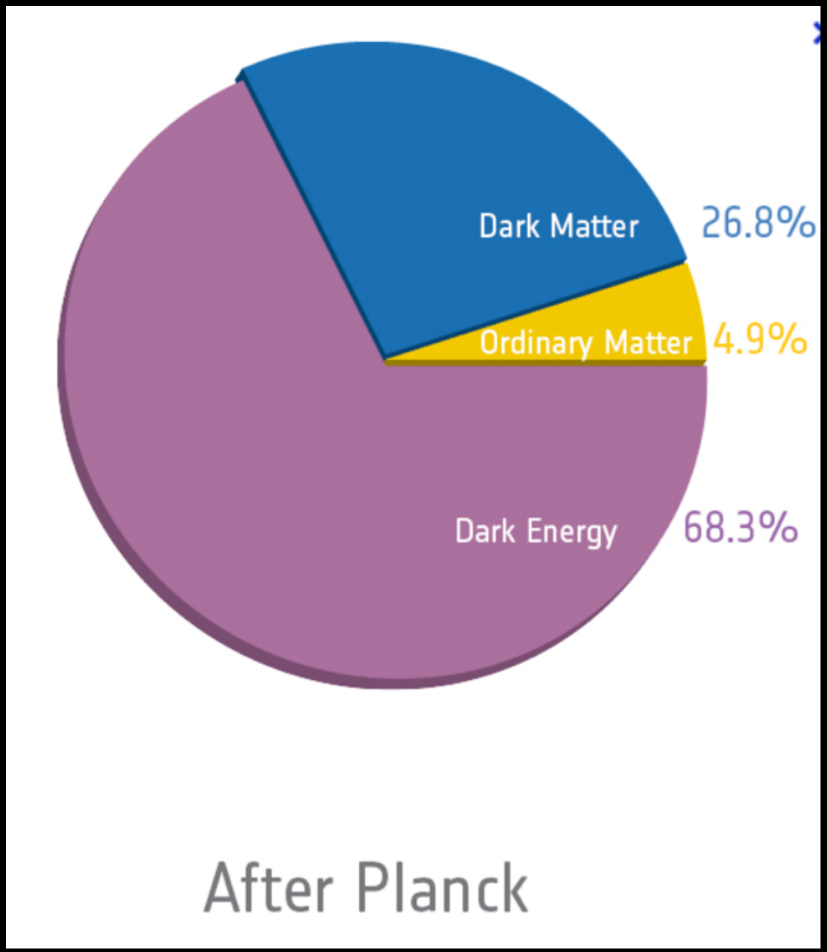

Cosmological and astrophysical observations

$\Omega_{DM} h^2 =$
0.1199 ± 0.0027

DM is …

Non-baryonic (BBN, CMB)

Collisionless (bullet cluster)

Stable on cosmological scales (or lifetime >> t_U ~13.8 Gyr)

Neutral

Massive

Cold or Warm (structure formation)

Not in conflict/excluded by DM experiments and cosmological data

…….not included in the Standard Model

Many candidates in Particle Physics → WIMPs, axions …

Additional assumptions for this talk:

- dark matter is a WIMP (GeV - TeV mass scale)
- WIMPs cluster in galaxies as dark halos (a main smooth halo and many subhalos)
- can pair annihilate or decay to produce SM particles
- accounts for the measured relic density

If DM is made of particles that interact among themselves and with SM particles we may hope to detect it. Two strategies:

1. DIRECT DETECTION (looks for energy deposited within a detector by the DM-nuclei scattering)

2. INDIRECT DETECTION (looks for WIMP annihilation (or decay) products)

2.1 Antimatter in the cosmic rays (antiprotons, antideuterons, positrons...)

2.2 Neutrinos (DM annihilation inside celestial bodies)

2.3 Photons (DM annihilation in the galactic halo(s))

+ complementary searches at colliders

Gamma-rays from WIMPs?

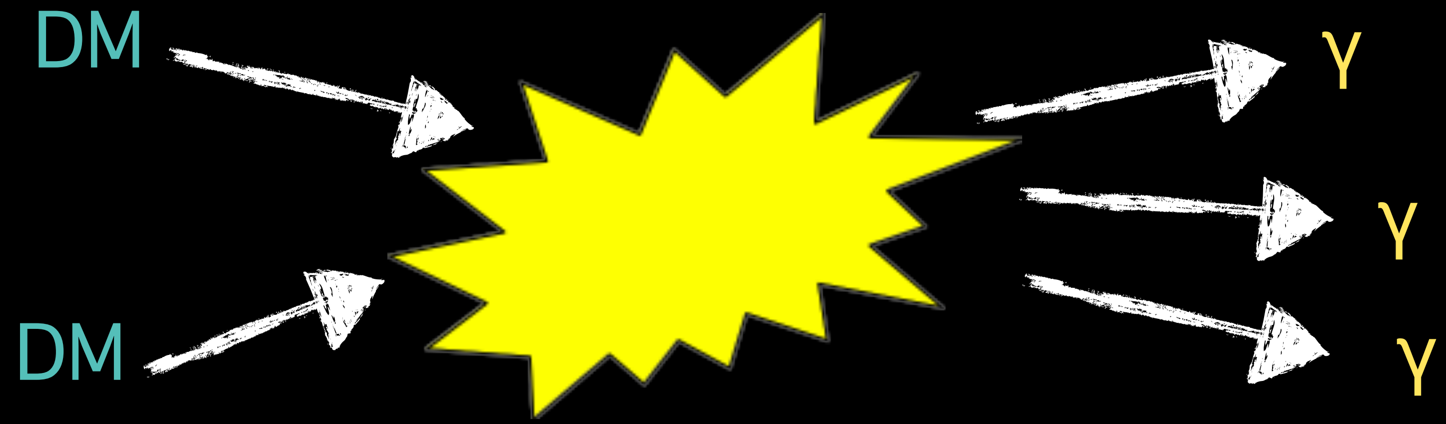

- Almost not absorbed/attenuated when propagating through halo
- Point directly to the sources: clear spatial signatures
- Clear spectral signatures to look for

but... need careful study of:

- diffuse background modelling
- properties of unresolved sources (number, distribution...)
- new type of sources?

Gamma-rays from WIMPs? - Annihilation processes

1. Prompt photons from DM annihilation:
   - Two-body annihilation into photons (gamma-ray lines)

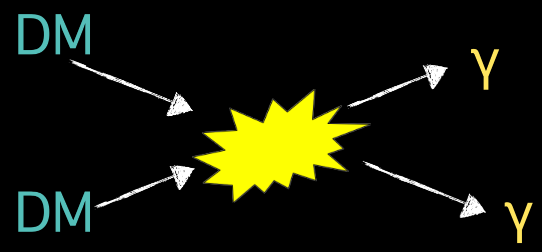

   - Photon production in hard process (bremsstrahlung of charged particles)

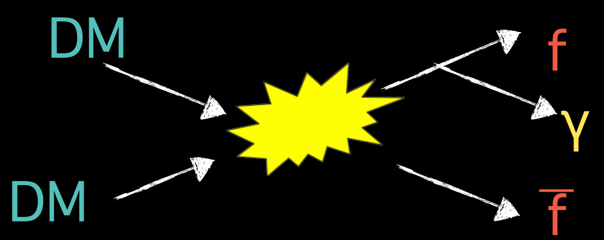

   - Two-photon decay of neutral pions $\pi^0 \rightarrow \gamma\gamma$ dumped by the hadronization chain of strongly interacting annihilation products (continuum)

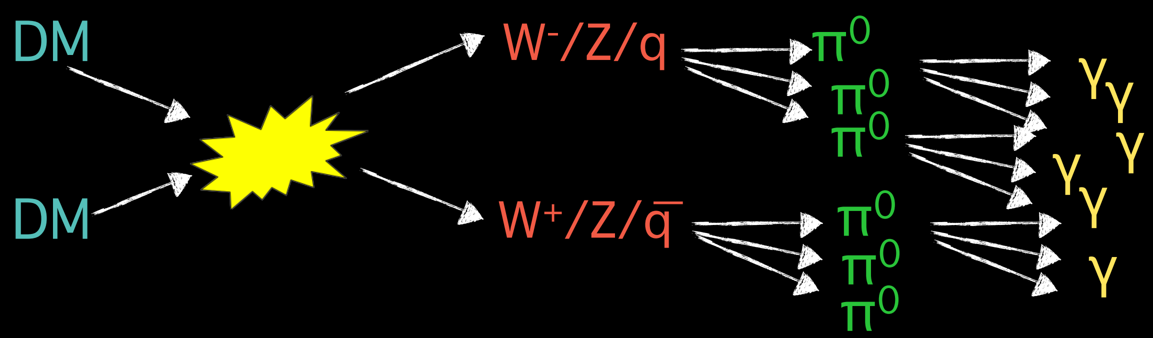

2. Secondary photons from radiative processes associated with stable, charged particles produced by DM annihilation or decay (electrons and positrons):

   e.g. inverse-Compton and synchrotron emission.

The γ-ray flux from DM annihilation is defined as the number of photons collected by a detector per unit of time, area, energy and solid angle:

$$\frac{d\Phi_\gamma}{dE_\gamma}(E_\gamma, \psi, \theta, \Delta\Omega) = \boxed{\frac{d\Phi_\gamma^{PP}}{dE_\gamma}(E_\gamma)} \times \boxed{J(\psi, \theta, \Delta\Omega)}$$

The γ-ray flux from DM annihilation is defined as the number of photons collected by a detector per unit of time, area, energy and solid angle:

$$\frac{d\Phi_\gamma}{dE_\gamma}(E_\gamma,\psi,\theta,\Delta\Omega) = \boxed{\frac{d\Phi_\gamma^{PP}}{dE_\gamma}(E_\gamma)} \times \boxed{J(\psi,\theta,\Delta\Omega)}$$

$$\boxed{\frac{d\Phi_\gamma^{PP}}{dE_\gamma} = \frac{1}{4\pi}\frac{\langle\sigma v\rangle}{2m_{DM}^2}\sum_i \frac{dN_\gamma^i}{dE_\gamma}B_i}$$

PARTICLE PHYSICS factor:

- $b\bar{b}$, $\mu^+\mu^-$, $\tau^+\tau^-$ final states
- Bi = 1
- spectra from Cembranos et al. PhysRevD.83.083507

Velocity averaged annihilation cross-section

Photon energy spectrum per annihilation

Characteristic Energy Spectrum

Important to:

- identify a DM signal
- determine the DM mass
- determine the annihilation process

The γ-ray flux from DM annihilation is defined as the number of photons collected by a detector per unit of time, area, energy and solid angle:

$$\frac{d\Phi_\gamma}{dE_\gamma}(E_\gamma,\psi,\theta,\Delta\Omega) = \boxed{\frac{d\Phi_\gamma^{PP}}{dE_\gamma}(E_\gamma)} \times \boxed{J(\psi,\theta,\Delta\Omega)}$$

$$\boxed{\frac{d\Phi_\gamma^{PP}}{dE_\gamma} = \frac{1}{4\pi}\frac{\langle\sigma v\rangle}{2m_{DM}^2}\sum_i \frac{dN_\gamma^i}{dE_\gamma}B_i}$$

PARTICLE PHYSICS factor:

- bb, $\mu^+\mu^-$, $\tau^+\tau^-$ final states
- Bi = 1
- spectra from Cembranos et al. PhysRevD.83.083507

$$\boxed{J(\psi,\theta,\Delta\Omega) = \int_0^{\Delta\Omega} d\Omega \int_{\mathrm{los}} \rho^2(\mathrm{r}(\mathrm{s},\psi,\theta))\mathrm{ds}}$$

ASTROPHYSICAL factor:

- Sensitivity to different DM halo profiles

Integration of the squared DM density at a distance s from the Earth in the direction along the l.o.s and in the observational cone of solid angle ΔΩ

γ-ray experiments relevant for DM searches

(GeV to TeV)

Space based: Fermi-LAT
(Pair conversion detector)

Effective area: O(1m^2)
Observation times: O(yr)
Energies: 0.02 - 300 GeV

Ground based: MAGIC, VERITAS, H.E.S.S.
(Atmospheric Cherenkov Telescopes)

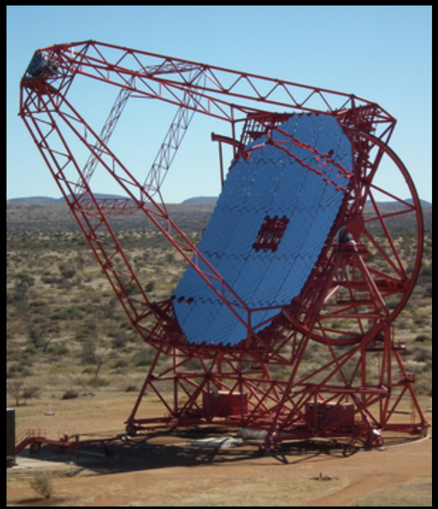

Effective area: O(1km^2)
Observation times: O(100hr)
Energies>100 GeV

γ-rays from DM: search targets

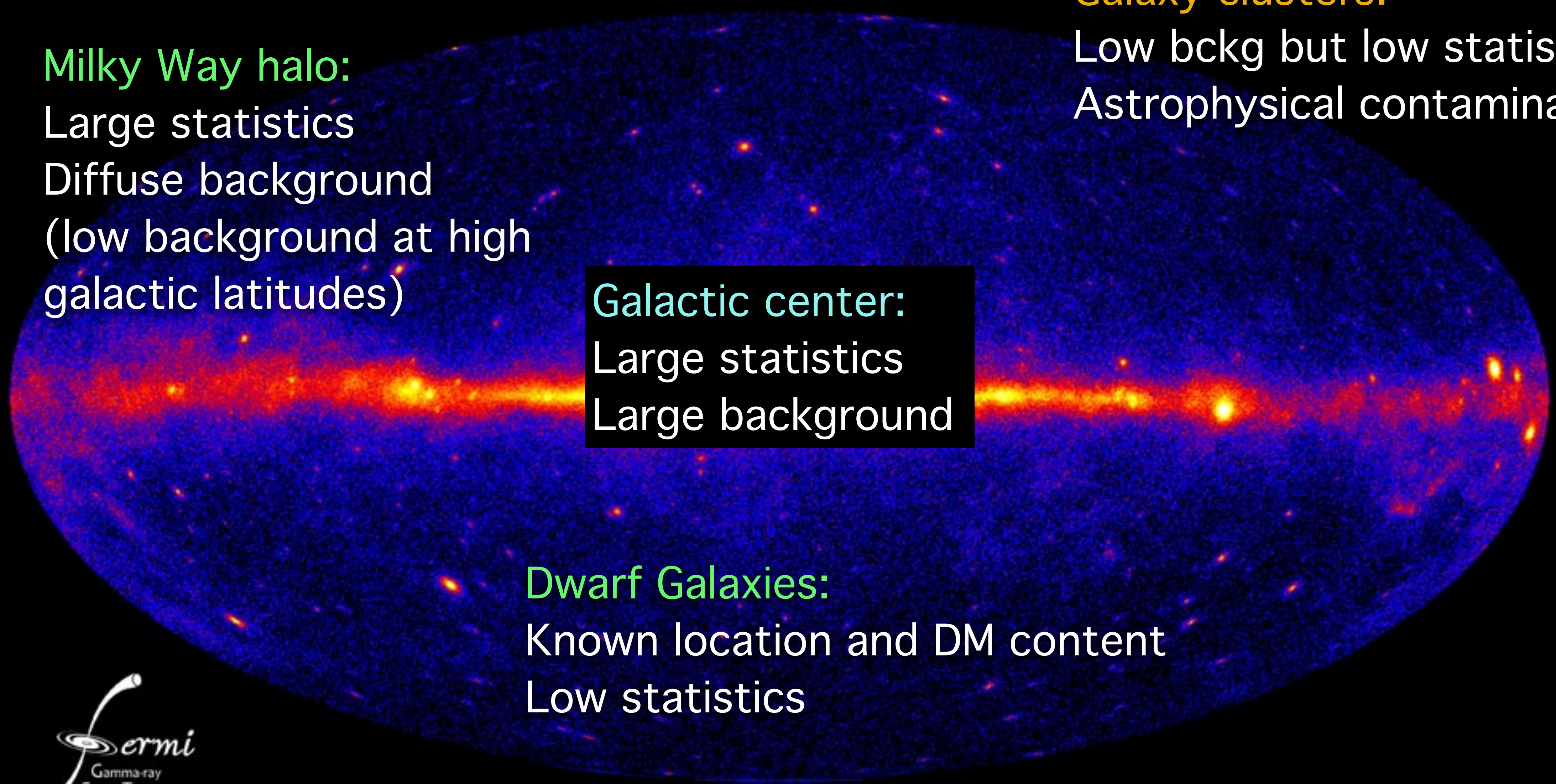

Galaxy clusters:
Low bckg but low statistics
Astrophysical contamination

Milky Way halo:
Large statistics
Diffuse background
(low background at high galactic latitudes)

Galactic center:
Large statistics
Large background

Dwarf Galaxies:
Known location and DM content
Low statistics

+ Spectral lines
Little or no astrophysical uncertainties, good source id, but low sensitivity because of expected small branching ratio

+ Isotropic background:
Large statistics, but astrophysics, galactic diffuse background

γ-rays from DM: search targets

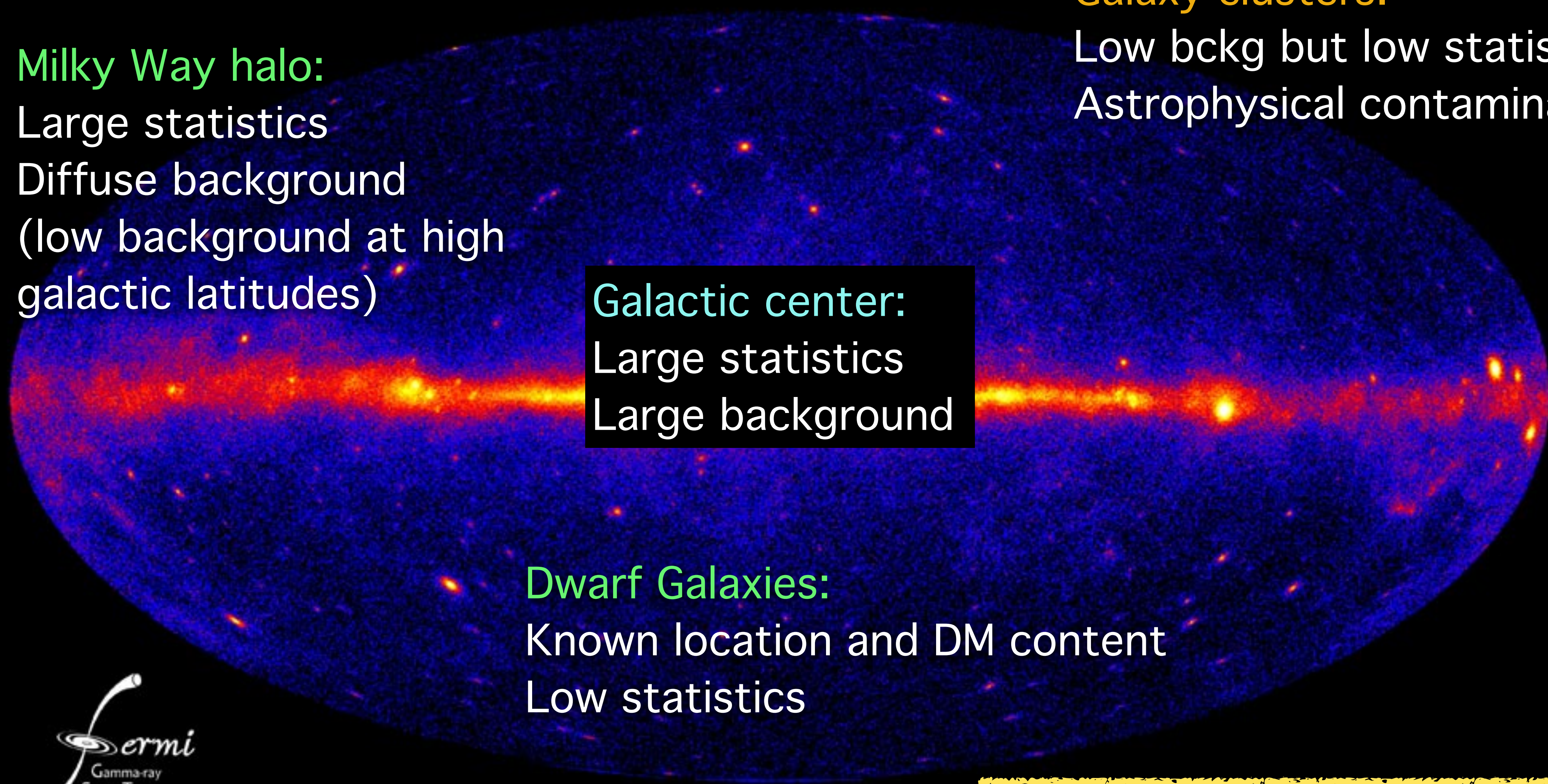

Galaxy clusters:
Low bckg but low statistics
Astrophysical contamination

Milky Way halo:
Large statistics
Diffuse background
(low background at high galactic latitudes)

Galactic center:
Large statistics
Large background

Dwarf Galaxies:
Known location and DM content
Low statistics

+ Spectral lines
Little or no astrophysical uncertainties, good source id, but low sensitivity because of expected small branching ratio

+ Isotropic background:
Large statistics, but astrophysics, galactic diffuse background

The extragalactic γ-ray emission (IGRB)

The excellent performances of Fermi-LAT have allowed the exploration for a DM component in the Milky Way, in extragalactic nearby objects, as well as in cosmological structures.

At high galactic latitudes, a faint γ-ray irreducible emission has been measured, and shown to be isotropic on large angular scales.

Fermi-LAT sky

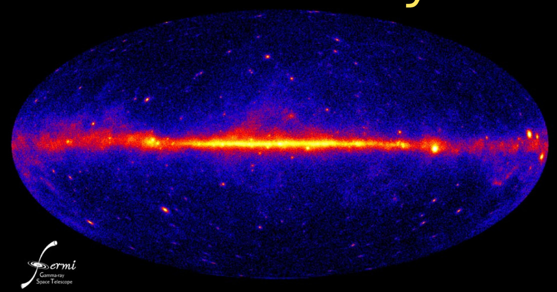

\-

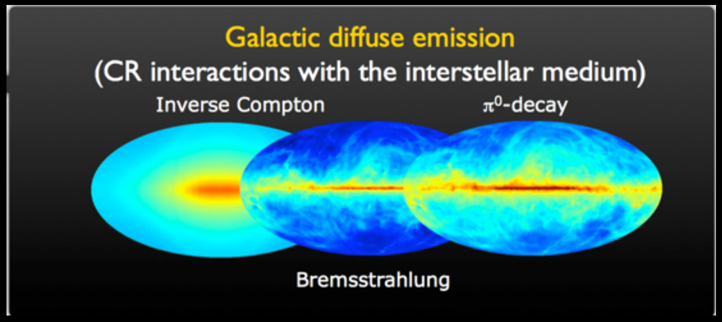

\-

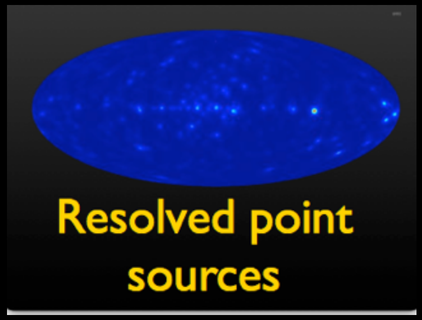

\-

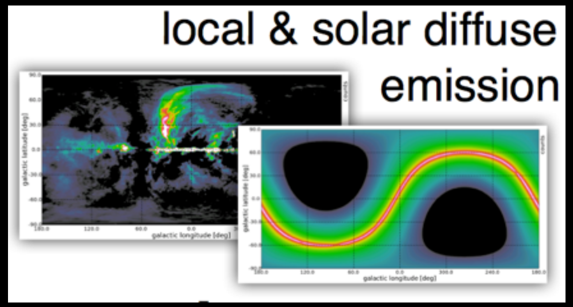

(+ CRs bkg)

=

- Undetected sources (blazars, AGNs, GRBs High-latitude pulsars, milli-second pulsars..)
- Diffuse processes (interactions of UHE cosmic rays with the EBL, Intergalactic shocks..)
- DARK MATTER???

γ-rays from DM and the IGRB

What can we learn about DM from IGRB?

1. spectral information

Energy range: 200 MeV – 100 GeV.
Observational region: |b|>10° (high-latitude).
Energy spectrum is featureless (a power law ($E^{-2.41}$))

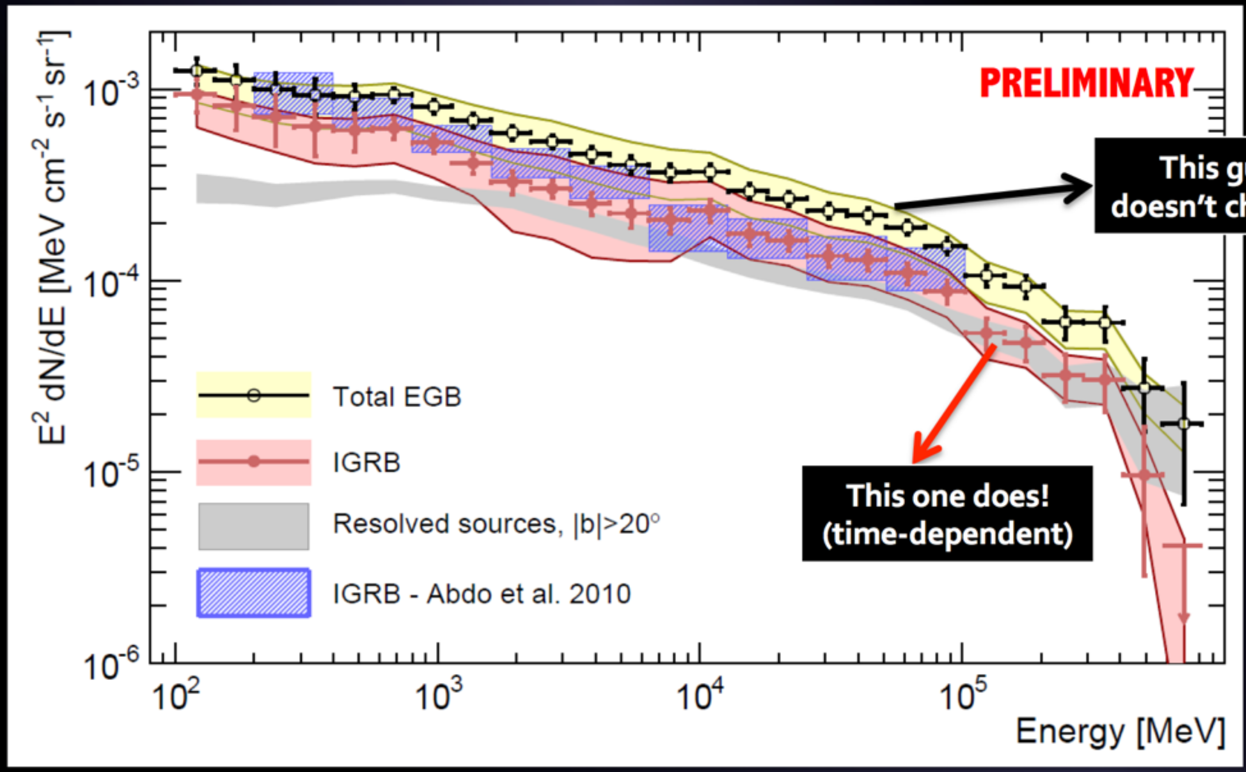

(from Sanchez-Conde @ APS meeting, Abdo et al., Phys.Rev.Lett. 104 (2010) 101101)

dark matter gives bumps, lines, cut-offs...
many astrophysical sources make power laws and may have exponential cut-offs but some astrophysical sources (e.g., pulsars) also give bumps

γ-rays from DM and the IGRB

What can we learn about DM from IGRB?

1. spectral information

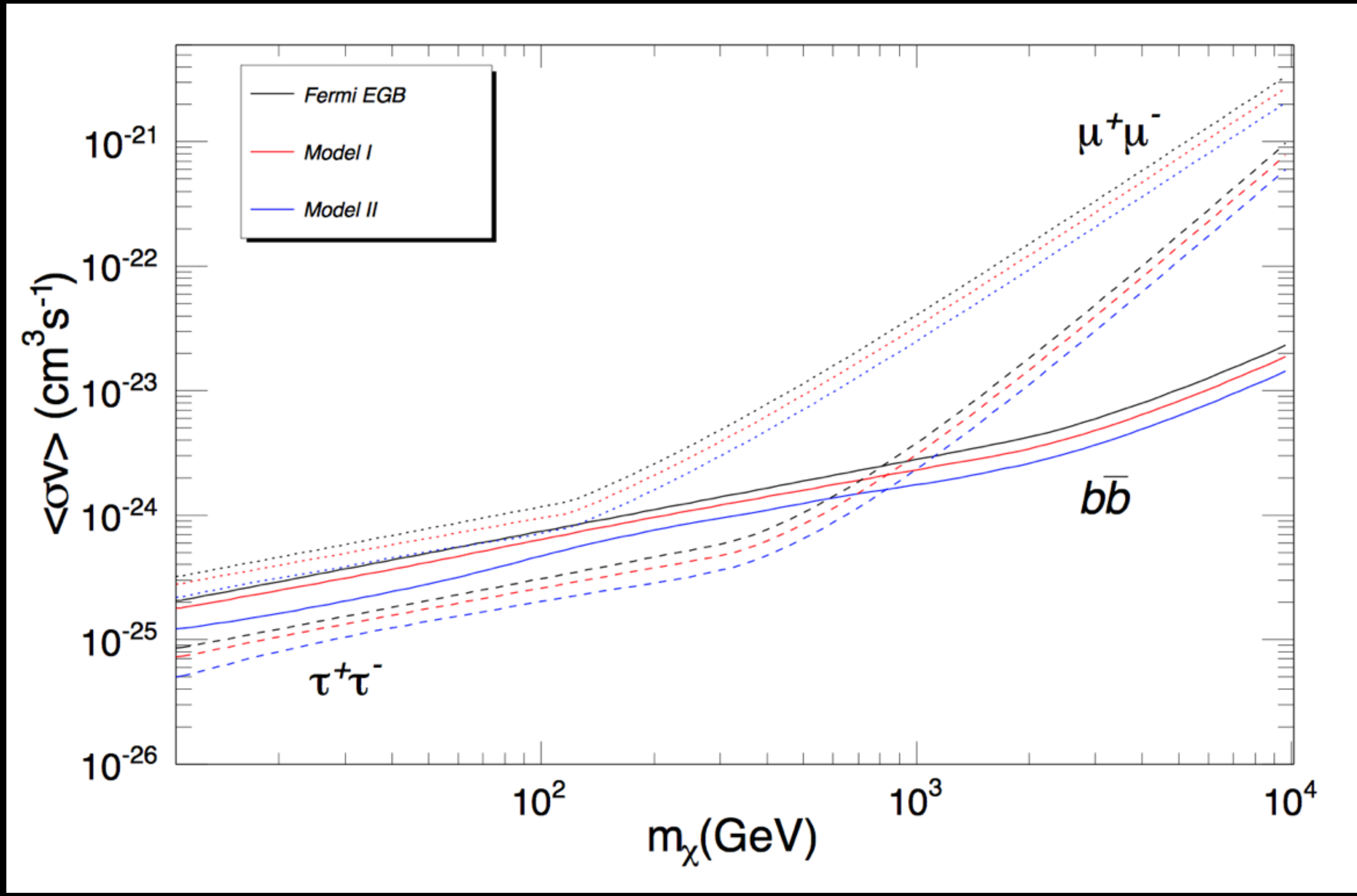

Calore, VDR and Donato, Phys.Rev. D85 (2012) 023004

From the intensity of IGRB we can obtain conservative upper limits on the DM annihilation cross section

γ-rays from DM and the IGRB

2. Spatial information: the IGRB is not perfectly isotropic.

The angular power spectrum (APS) characterises its intensity fluctuations as a function of angular scale.

- diffuse emission that originates from one or more unresolved source populations will contain fluctuations on small angular scales due to variations in the number density of sources in different sky directions
- the amplitude and energy dependence of the anisotropy can reveal the presence of multiple source populations and constrain their properties

γ-rays from DM and the IGRB

2. Spatial information: the IGRB is not perfectly isotropic.
   The angular power spectrum (APS) characterises its intensity fluctuations as a function of angular scale.

   - diffuse emission that originates from one or more unresolved source populations will contain fluctuations on small angular scales due to variations in the number density of sources in different sky directions

   - the amplitude and energy dependence of the anisotropy can reveal the presence of multiple source populations and constrain their properties

The study of the APS is interesting because:

- Complementary with the analysis of the intensity energy spectrum
- Depends on the spatial distribution of sources, alternative to the study of point sources
- If ascribable to DM sources may be an important signature worth to be explored

Anisotropies in the γ-ray sky

The Fermi-LAT has already reported the detection of a non-zero angular power spectrum (APS) above the noise level in the multipole range $l \sim 155 \div 504$, corresponding to an angular scale $\lesssim 2°$

It is expected that the statistical properties of the DM distribution in galactic and extragalactic space are different from those of standard astrophysical objects.

Anisotropies in the γ-ray sky

The Fermi-LAT has already reported the detection of a non-zero angular power spectrum (APS) above the noise level in the multipole range $l \sim 155 \div 504$, corresponding to an angular scale $\lesssim 2°$

It is expected that the statistical properties of the DM distribution in galactic and extragalactic space are different from those of standard astrophysical objects.

We discuss:

i) the intrinsic uncertainty due to the extrapolation to short distances of the DM distribution determined from numerical simulations;

ii) the different signatures in the APS in connection with the various density profiles (cored and cuspy).

Calore, VDR, Di Mauro, Donato, Herpich, Macciò, Maccione, Mon.Not.Roy.Astron.Soc. 442 (2014) 1151-1156

Angular power spectrum

The angular power spectrum (APS) C_ℓ of an intensity map I (Ψ) where Ψ is the direction in the sky, is given by the coefficients:

$$C_\ell = \frac{1}{2\ell+1} \sum_{|m|<\ell} |a_{\ell m}|^2$$

with the a_{lm} determined by expanding the sky map in spherical harmonics, after subtracting the average value of the intensity over the region of the sky considered:

$$I(\Psi) = \frac{\mathrm{d}\Phi}{\mathrm{d}E}(\Psi) - \langle\frac{\mathrm{d}\Phi}{\mathrm{d}E}(\Psi)\rangle = \sum_{\ell=0}^{\infty} \sum_{m=-\ell}^{m=\ell} a_{\ell m} Y_{\ell m}(\Psi).$$

The APS gives the measure of a signal correlation between two angular scales, and, in turns, between two spatial scales.

For ex.: the APS at multipoles, for example, $l > 500$ probes the DM distribution at $R < \pi/500 \cdot 8.5$ kpc ~ 40 pc.

Angular power spectrum

The angular power spectrum (APS) C_ℓ of an intensity map I (Ψ) where Ψ is the direction in the sky, is given by the coefficients:

$$C_\ell = \frac{1}{2\ell+1} \sum_{|m|<\ell} |a_{\ell m}|^2$$

with the a_{lm} determined by expanding the sky map in spherical harmonics, after subtracting the average value of the intensity over the region of the sky considered:

$$I(\Psi) = \frac{\mathrm{d}\Phi}{\mathrm{d}E}(\Psi) - \langle \frac{\mathrm{d}\Phi}{\mathrm{d}E}(\Psi) \rangle = \sum_{\ell=0}^{\infty} \sum_{m=-\ell}^{m=\ell} a_{\ell m} Y_{\ell m}(\Psi).$$

The APS gives the measure of a signal correlation between two angular scales, and, in turns, between two spatial scales.
For ex.: the APS at multipoles, for example, l > 500 probes the DM distribution at R < π/ 500 · 8.5 kpc ~ 40 pc.

The study of the APS at l ≳ 500 requires to know the DM profile at scales much below the resolution (~200 pc) of current state of the art numerical simulations for structure formation

DM halos' profiles: cusped or cored?

To determine the γ-ray emission a special rôle is devoted to the radial density profile of the DM halo ρ(r), with particular attention to the central region.

$$\rho(r) = \rho_0 \left[\left(\frac{r}{R_c}\right)\left(1+\frac{r}{R_c}\right)^2\right]^{-1} \qquad \text{(NFW)}$$

$$\rho(r) = \rho_0 \exp\left(-\frac{2}{\alpha_E}\left[\left(\frac{r}{R_s}\right)^{\alpha_E}-1\right]\right) \qquad \text{(Ein)}$$

$$\rho(r) = \rho_0 \exp\left(-\lambda\left[\ln\left(1+\frac{r}{R_\lambda}\right)\right]^2\right) \qquad \text{(MS)}$$

Einasto (1965), Trudy Inst. Astrofiz. Alma-Ata 51, 87
2 Stadel et al., MNRAS (2009) 398 (1): L21-L25.
3 Navarro,Frenk and White, Astrophys.J. 462 (1996) 563-575

DM halos' profiles: cusped or cored?

$$\rho(r) = \rho_0 \left[\left(\frac{r}{R_c}\right) \left(1 + \frac{r}{R_c}\right)^2 \right]^{-1} \qquad \text{(NFW)}$$

$$\rho(r) = \rho_0 \exp\left(-\frac{2}{\alpha_E} \left[\left(\frac{r}{R_s}\right)^{\alpha_E} - 1 \right] \right) \qquad \text{(Ein)}$$

$$\rho(r) = \rho_0 \exp\left(-\lambda \left[\ln\left(1 + \frac{r}{R_\lambda}\right) \right]^2 \right) \qquad \text{(MS)}$$

Einasto (1965), Trudy Inst. Astrofiz. Alma-Ata 51, 87
2 Stadel et al., MNRAS (2009) 398 (1): L21-L25.
3 Navarro,Frenk and White, Astrophys.J. 462 (1996) 563-575

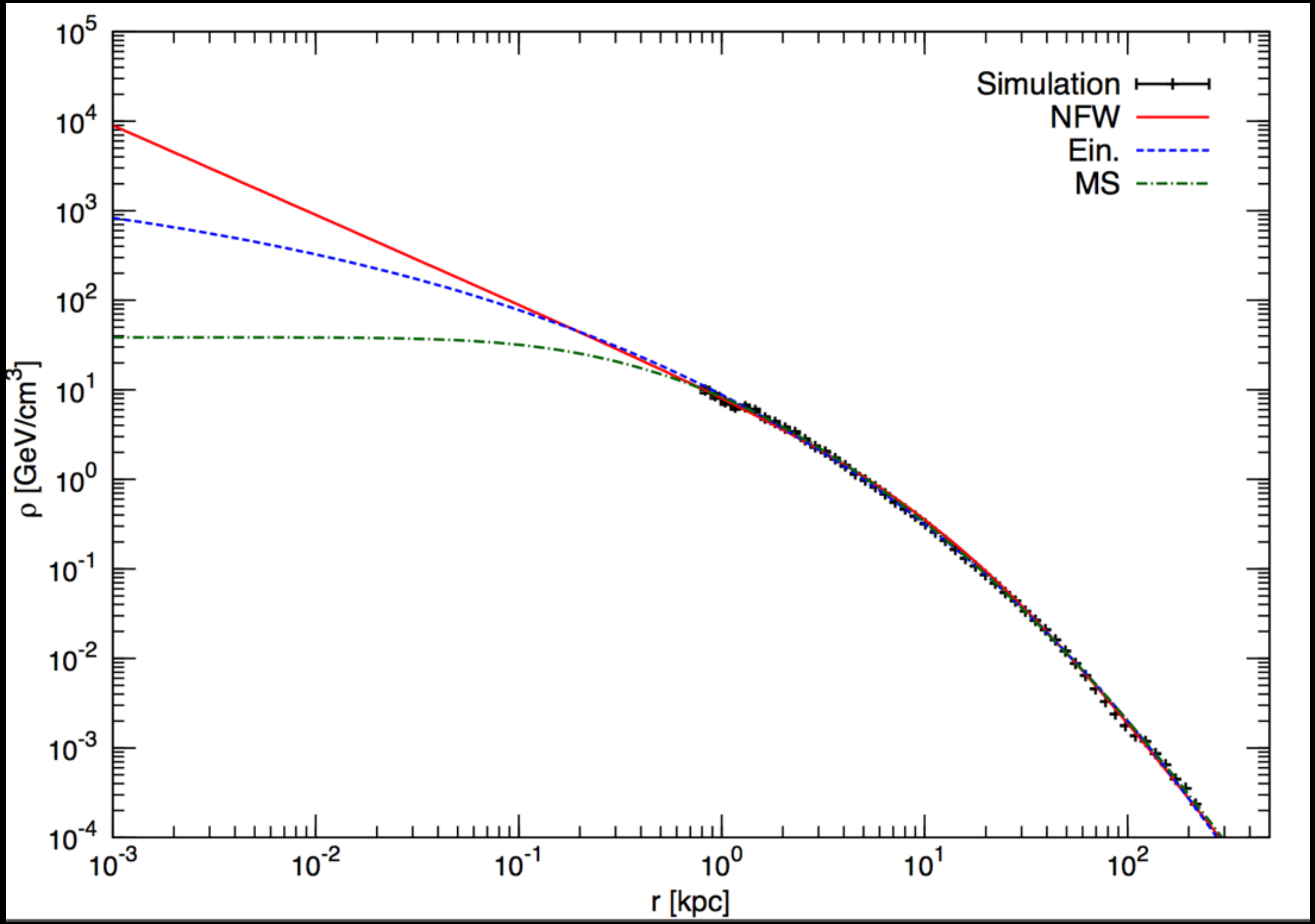

N-body counterparts of the MaGICC (Making Galaxies in a Cosmological Context) simulations suite; Stinson et al. (2013) Di Cintio et al. (2014)

Galaxy with a virial mass of 1.48 × $10^{12} M_\odot$

when extrapolated below the resolution limit of cosmological simulations, different profiles predict very different central densities!

We have computed the space distribution of the γ-ray emission from DM annihilation based on the g15784 halo simulation

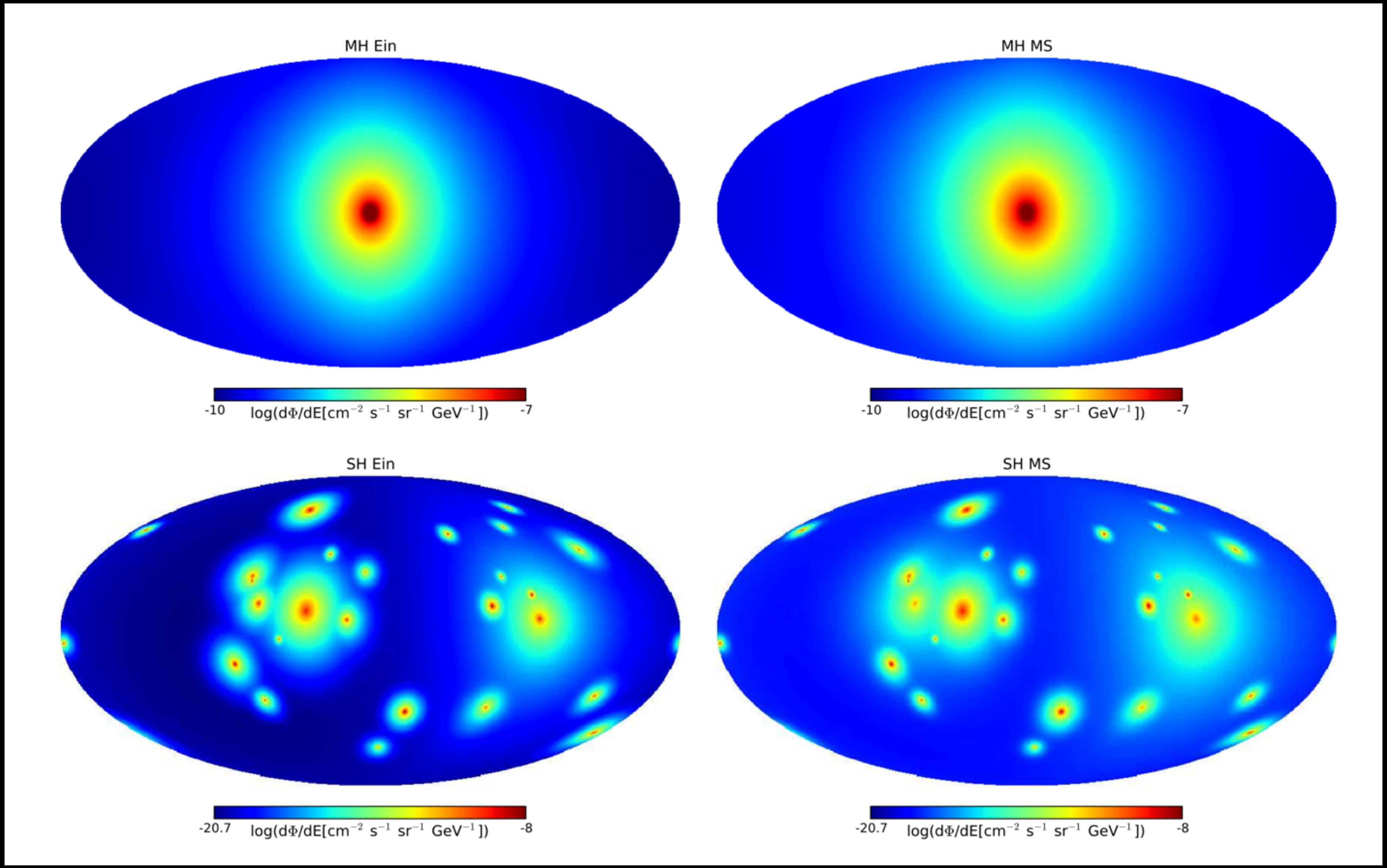

γ-ray emission at E_γ=4 GeV, from the annihilation of m_{DM}= 200 GeV, $b\bar{b}$ channel

The γ-ray intensity maps and their power spectra have been generated by using the HEALPix software (Górski et al. 2005).

Number of pixels of the map is $N_{pixel} = 12 \cdot 2^{2k}$

Solid angle of one pixel of the map is $\Delta\Omega = 4\pi/N_{pixel}$

We use k=13, so that $\Delta\Omega = 1.56 \cdot 10^{-8}$ sr for a corresponding scale of about 1 pc, and k=9 for the Monte Carlo

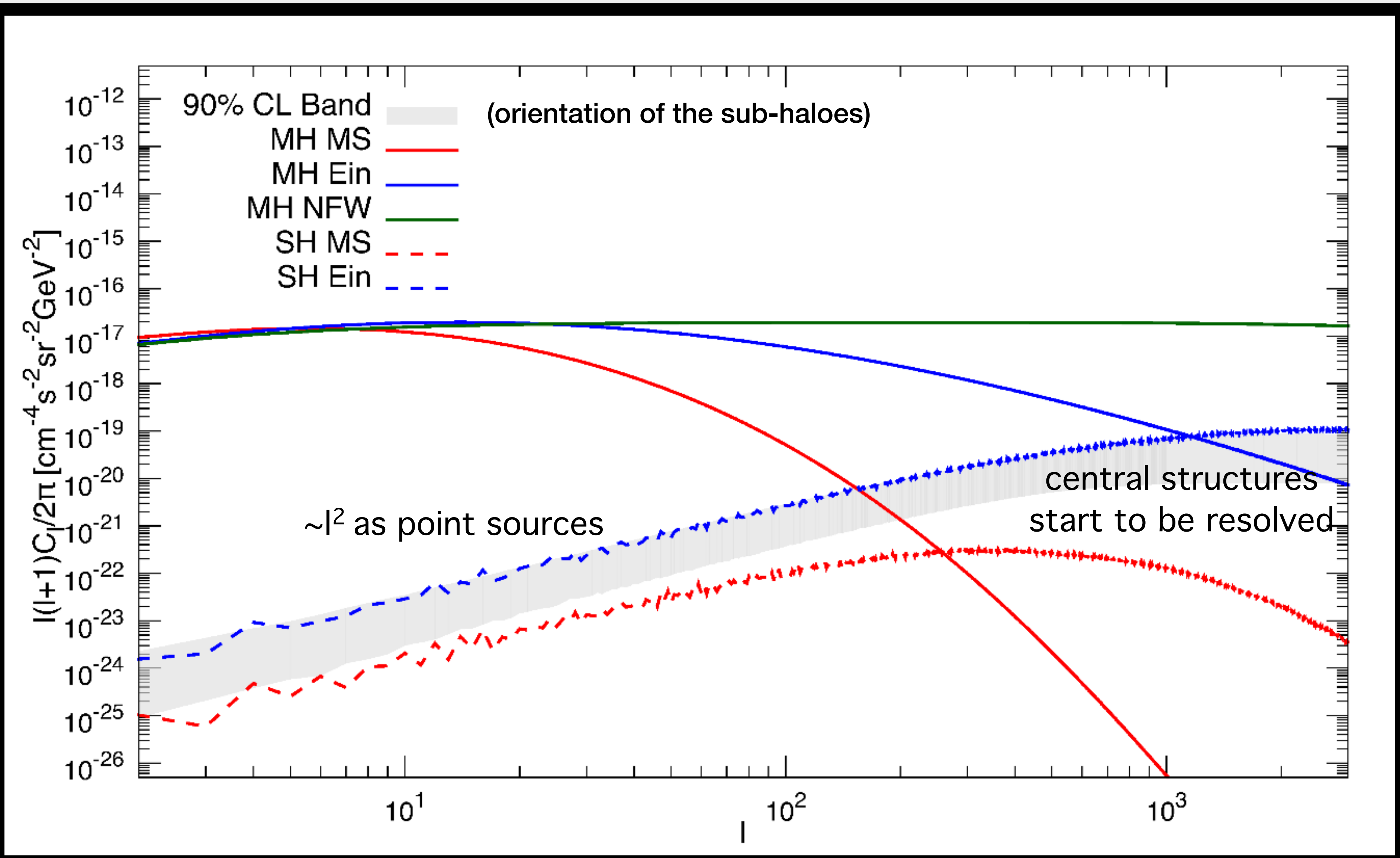

1. MAIN HALO:
   - Peaked Einasto profile: more power at small radial scales (high l), both smooth halo and subhalos
   - The two profiles give comparable APS only for l ≲10
   - At l=100 the Einasto APS is ~ 2 orders of magnitude higher than the MS
   - At l=1000(~ 30 pc), the main halo within the MS profile does not contribute any longer to the anisotropy of the sky, while the Einasto profile still provides a sizable APS
2. SUBHALOS:
   - the APS is much milder in the case of the cored MS profile than the Einasto one.
   - Einasto profile is more concentrated in the center: the clumps, appearing more as point-like, inject more power at all scales.

Effect of sub-haloes smaller than those of the g15784 simulation on the APS.
Monte Carlo simulation based on the Aquarius Aq-A-1 results
(analytical fits in Pieri et al. Phys.Rev. D83 (2011) 023518)

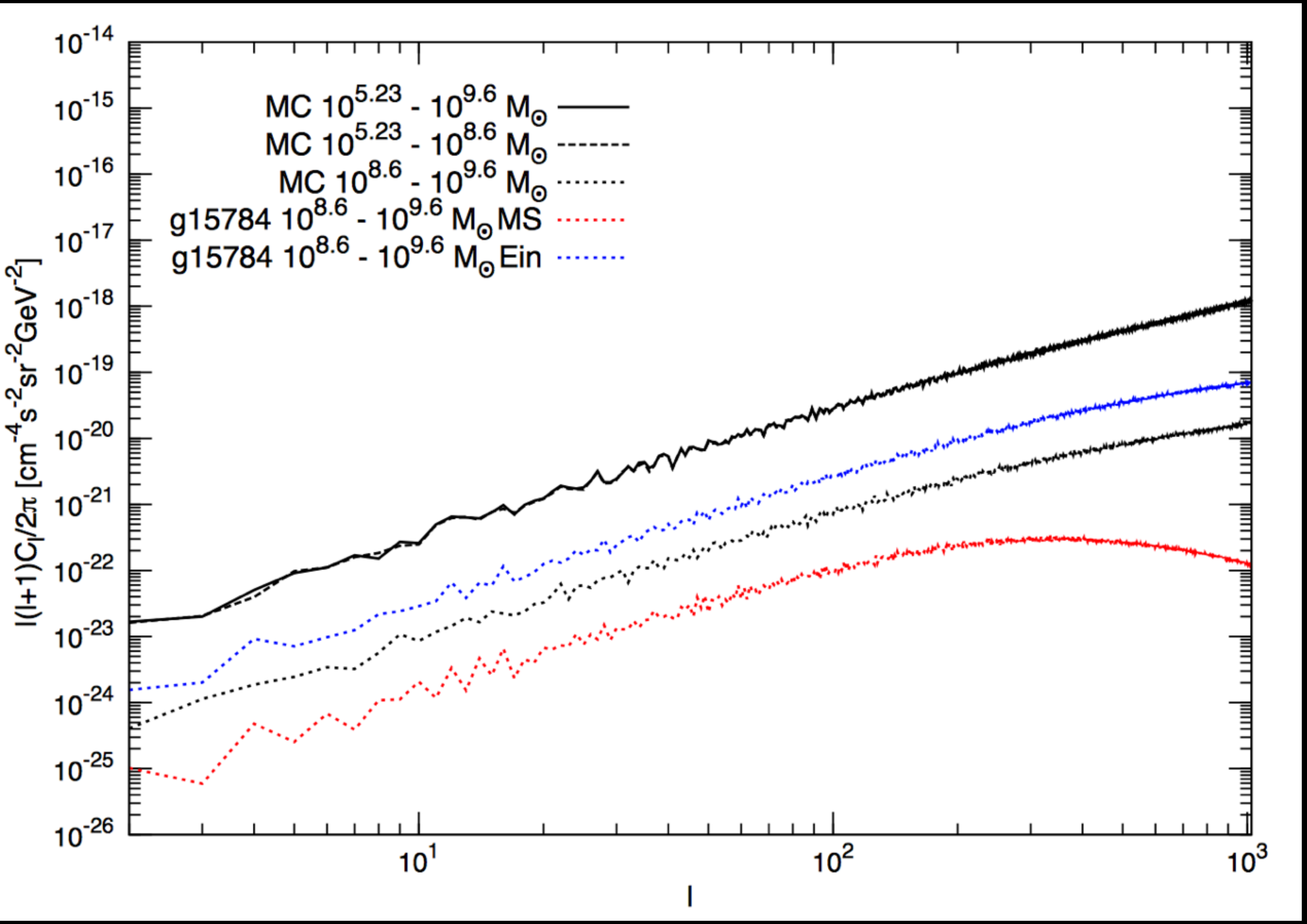

The more massive haloes lead to the flattening of the APS at large multipoles, as expected, while the contribution of the sub-structures lighter than $10^{8.6}M_\odot$ is slightly more Poisson-like, and dominates the total APS, which results to be more intense because of this additional component.

Conclusions

- We have calculated the intensity APS of the γ-ray flux from DM annihilation in the halo of a Milky Way like galaxy
- The simulated galactic halo and its subhalos can be equally well interpreted in terms of a peaked Einasto as well as an asymptotically cored MS radial DM profile (though leading to very different predictions for the γ-ray intensity APS)
- The DM halo and subhalos, when interpreted in terms of the peaked Einasto profile, yield much higher APS at small radial scales (high l) than the cored MS $\rho(r)$
- We underline the caution in adopting extrapolated DM profiles when dealing with anisotropy searches, and emphasize the need for a better knowledge of the distribution of the DM in its clustered structures, especially taking into account the possible effects of baryonic matter
- The study of high-multipoles anisotropies - achievable by the next generation of Cherenkov telescopes such as CTA - might help in the debate about the real shape of the DM distribution in the center of the galaxies, and in particular of the Milky Way

Conclusions

- We have calculated the intensity APS of the γ-ray flux from DM annihilation in the halo of a Milky Way like galaxy
- The simulated galactic halo and its subhalos can be equally well interpreted in terms of a peaked Einasto as well as an asymptotically cored MS radial DM profile (though leading to very different predictions for the γ-ray intensity APS)
- The DM halo and subhalos, when interpreted in terms of the peaked Einasto profile, yield much higher APS at small radial scales (high ℓ) than the cored MS $\rho(r)$
- We underline the caution in adopting extrapolated DM profiles when dealing with anisotropy searches, and emphasize the need for a better knowledge of the distribution of the DM in its clustered structures, especially taking into account the possible effects of baryonic matter
- The study of high-multipoles anisotropies - achievable by the next generation of Cherenkov telescopes such as CTA - might help in the debate about the real shape of the DM distribution in the center of the galaxies, and in particular of the Milky Way

Thank you!